Surfactant-stabilized strained Ge cones on Si(001)

M. Horn-von Hoegen,* A. Al Falou, B. H. Müller, U. Köhler, L. Andersohn, B. Dahlheimer, and M. Henzler
Institut für Festkörperphysik, Universität Hannover, Appelstrasse 2, 30167 Hannover, Federal Republic of Germany
(Received 26 July 1993)

The formation of circular cone-shaped Ge islands (12° cones) has been observed for the growth of eight monolayers of Ge on Si(001) at 700 °C using Sb as a surfactant. The Ge cones are strained and grow pseudomorphically, adopting the Si lattice constant. They have a tilt angle of 12° and are composed of [117]-, [105]-type, and all intermediate facets. The island-size distribution is peaked around a typical size of ~300–400 Å, which results from a formation process under equilibrium conditions for diffusion of the Ge atoms. Growth at lower temperatures down to 300 °C with Sb as a surfactant results in epitaxial but very rough Ge films which show a high degree of disorder.

I. INTRODUCTION

The use of surfactants in order to force layer growth of different and especially nonlattice matching materials has recently attracted much attention.[1–3] The growth of Ge on Si is the subject of intense studies due to the potential benefits for semiconductor technology. Short-period superlattices, for example, may allow direct optical transitions by a zone folding effect and thus Si-based optoelectronic devices.[4] Heterobased bipolar devices are already competing in speed with GaAs technology.[5]

Although it is generally accepted that certain surfactants allow Ge films to grow on Si in a layer-by-layer mode, the situation may be very different on an atomic scale for the pseudomorphic growth regime prior to the generation of misfit-relieving defects. The film usually roughens in order to relieve the misfit-related strain by partial lateral relaxation towards its own lattice constant. A flat and continuous film would not allow for this kind of relaxation because all Ge atoms have to take lattice positions given by the Si lattice parameter. This roughness may even be enforced in the presence of a surfactant: the growth of three monolayers [one monolayer (ML)$=6.78\times10^{14}$ atoms cm^{-2}] of Ge on Si(111) results in flat Ge films with a (5×5) reconstruction,[6] whereas a coevaporation of Sb results in the formation of one-atom-wide trenches in the Ge film in order to relieve strain.[7] Up to a thickness of eight monolayers of Ge the surface has completely roughened by the formation of very small micropyramids (diameter ~100 Å) mainly composed of [113]-type facets.[8] The Ge in these micropyramids relaxes partially towards its own bulk lattice parameter without generation of defects. This strain-relief mechanism via the formation of a microrough surface has also been observed for a wide range of temperatures (300–600 °C) for the growth of Ge on Si(001) using Sb as a surfactant.[9] The use of As as a surfactant results in a criss-cross arrangement of small Ge dimer rows, most of them only one dimer wide.[10] Only the generation of misfit-relieving defects smoothens the surface allowing nearly perfect layer-by-layer growth. Hut clusters, which are found during the growth of Ge on Si(001) without surfactants,[11] are also formed by a similar mechanism of strain relief in the pseudomorphic growth regime prior to the generation of defects.

The surface morphology during this rough growth stage is additionally influenced by the selective change of the growth kinetics caused by the surfactant.[12] At low temperatures a disordered structure is expected, with increasing temperature a higher regularity of the film, which is still rough in order to relieve strain, may be observed. At very high temperatures the surfactant will lose its kinetic limiting behavior, and the surface free energy, which is affected by the surfactant, becomes more and more important for the surface morphology.

We have investigated this transition from kinetically hindered growth to growth under equilibrium conditions for the pseudomorphic growth regime of Ge on Si(001) using Sb as a surfactant. The influence of deposition temperature on the surface morphology for substrate temperatures ranging from 500 °C to 800 °C has been studied using surface-sensitive methods. We present this in a combined spot profile analyzing low-energy electron diffraction (SPA-LEED) and scanning tunneling microscopy (STM) study.

SPA-LEED is able to provide quantitative and qualitative information about surface morphology not only after film growth but also at elevated substrate temperatures during deposition. Determination of parallel and vertical (layer distance) lattice parameters with an accuracy of 0.005 Å allows observation of the strain relaxation of the growing film. Not only the superstructure but also size distributions of islands or terraces are available on a length scale from a few atoms up to 2000 Å. Surface roughness is determined by the energy dependence of spot positions (facets) or the spot profile (islands) in a quantitative way. STM allows the easy and direct determination of the local geometry of islands on an atomic scale. Island-size distributions as well as roughness could be estimated. Combination of both methods allows the determination of nearly all parameters concerning the surface morphology.

We report the formation of flat cone-shaped circular islands (12° cones) as the equilibrium configuration of the Sb-covered Ge film at high temperatures (700 °C). At 600–650 °C a rough surface composed of terraces with a

size of 8×8 atoms is observed. At lower temperatures down to 300 °C the surface is still perfectly epitaxial, but with a highly irregular terrace structure.

II. EXPERIMENT

The experiments were performed in two separate standard ultrahigh vacuum (UHV) chambers each with a base pressure of 8×10^{-11} mbar. One is equipped with a SPA-LEED,[13] a cylindrical mirror analyzer (CMA) for Auger measurements, and a quadrupole mass spectrometer. Using a grazing electron gun in a geometry similar to reflection high-energy electron diffraction experiments,[14] the films could be grown with simultaneously taking data. STM experiments have been carried out in a second chamber equipped with a four-grid LEED optic, a CMA for Auger measurements, and a quadrupole mass spectrometer. Samples have been prepared *in situ* in each chamber thus avoiding a transfer through air or by a UHV suitcase.

Ge is evaporated from an electron-beam-heated graphite crucible, with the flux monitored by a quartz microbalance. The crucible is held in a water-cooled copper shroud, mounted together with a shutter on a 2.75-in. flange. Ge ions were deflected by an electrostatic field. Sb is evaporated from a quartz crucible, also equipped with shutter and microbalance.

The Si substrates were cut from well-oriented (001) wafers, with an orientation better than 0.2° within the ideal (001) plane. After degassing the samples at 600 °C for one night in the load-lock chamber, the native oxide is removed by a short flash to 1050 °C. No contamination was detected by Auger spectroscopy (sensitivity for C relative to Si is better than 1:1000). The Ge film of usually 8 ML coverage has been grown with a rate of 0.5 ML/min.

The Sb flux is not exactly known, but it is high enough to establish the saturation coverage of nearly 1 ML for temperatures below 600 °C. Significant desorption of Sb at 700 °C and higher temperatures reduces the stationary Sb coverage to about 0.3–0.5 ML, as determined by Auger spectroscopy. The observed surface morphology strongly depends on the Sb coverage at this high temperature (and thus the Sb flux) and is thoroughly addressed elsewhere.[15]

III. LEED RESULTS

Growth of 8 ML of Ge by using Sb as a surfactant at 700 °C results in quite surprising LEED patterns, for example, the "half-moon"-shaped (10) spot at 76 eV electron energy shown in Fig. 1. The (00) spot is redistributed into a circular intensity ring, here shown at 92 eV in Fig. 2. All integer-order spots of the LEED patterns show this intensity ring too. The diameters of these rings depend on electron energy and the integer order of the LEED spot as shown in Figs. 3(a)–3(c). At the in-phase condition of scattering the spots are sharp and bright. This reflects the perfect epitaxial growth of the Ge with all atoms on lattice sites. The scattering conditions for the LEED patterns shown in Fig. 3 are plotted as dashed circle segments in Fig. 4 in reciprocal space of the (001)

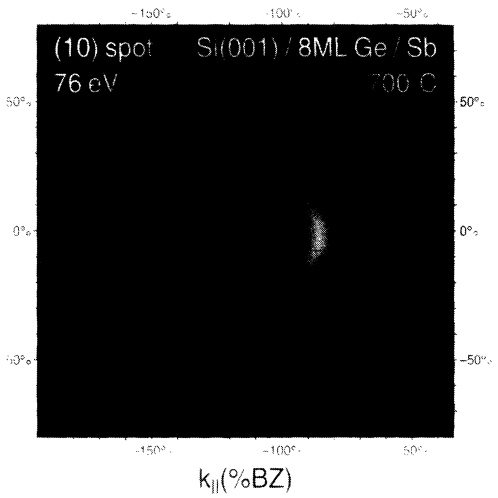

FIG. 1. Half-moon-shaped (10) spot at 74 eV after growth of 8 ML of Ge on Si(001) at 700 °C with Sb as a surfactant.

surface. On the left-hand side of Fig. 4 a cut in the [100] direction of the reciprocal space is shown and on the right-hand side a cut in the [110] direction is shown. The in-phase conditions for scattering are marked by closed dots. Due to the two different step geometries for the [110] directions[16] the in- and out-of-phase conditions are not well defined for the (10) rod and are marked by the open dots.[17]

The nature behind the LEED patterns is illuminated by taking a closer look at the behavior of the (00) spot. The diameter of the ring decreases with decreasing deviations from the in-phase condition at 72 eV, as shown in Fig. 5 in a series of two-dimensional (2D) scans at different electron energies. By decreasing the energy even more the diameter increases again. Above 82 eV, the ring shows a fourfold symmetry with slightly increased intensity towards the (11) spots. Below 54 eV a behavior

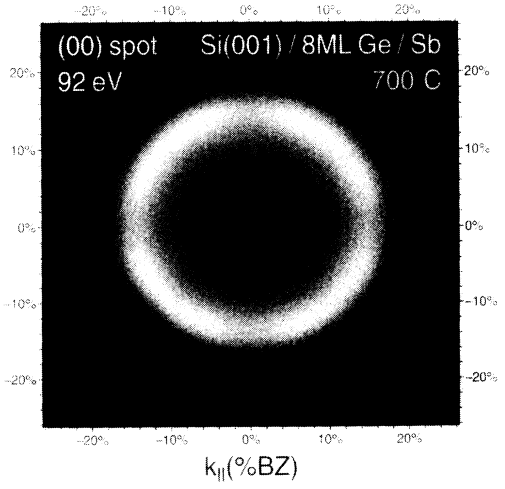

FIG. 2. The (00) spot at 90 eV shows a ringlike structure. The fourfold intensity variation on the perimeter is caused by dynamic scattering effects.

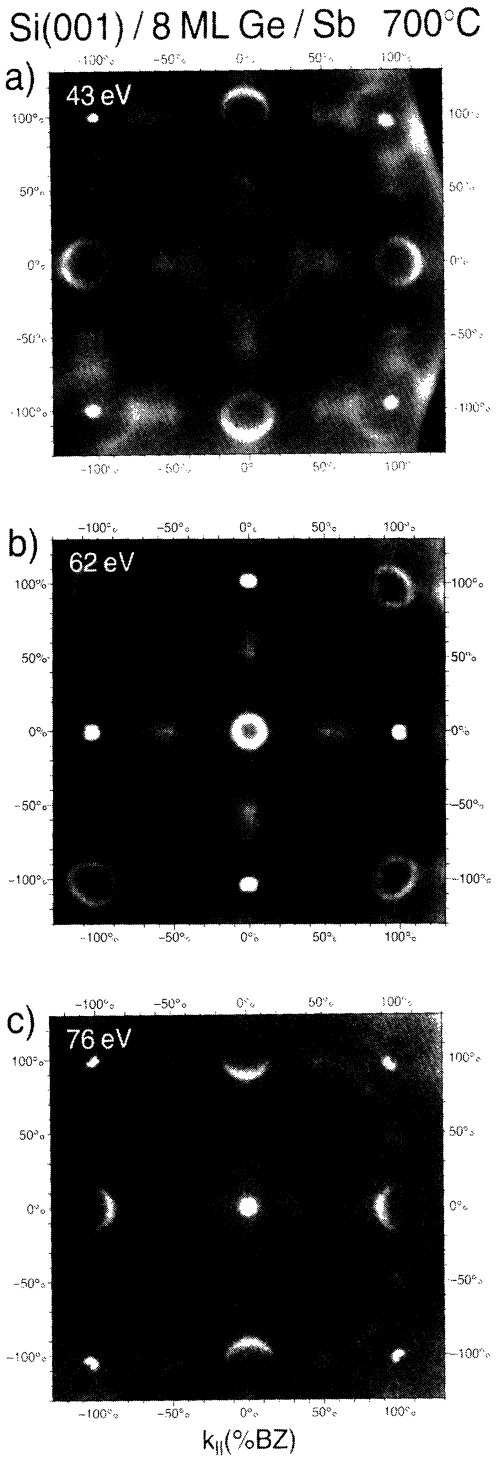

FIG. 3. All integer-order spots of the LEED patterns show the ringlike behavior. The diameter of the rings depends on the electron energy. (a) At 43 eV the (11) spots are bright and sharp due to their in-phase condition. The (10) spots show a ring as well as the (00) spot. The four faint spots in the center of the image are caused by an additional double periodicity on the [117] facets of the 12° cones. (b) At 62 eV the (10) spots have their in-phase condition. The (11) spots show a ring as well as the (00) spot. The size of the ring around the (00) spot has decreased. (c) At 76 eV the (00) spot is close to the in-phase condition. The (10) spots show a half-moon-shaped form caused by variations of the form factor of scattering.

rotated by 45° is observed. The LEED patterns of a stepped surface (i.e., all atoms on lattice sites) must have a point symmetry with respect to the bulk Bragg conditions,[18] which are the in-phase conditions for surface scattering. Since the azimuthal intensity dependence is rotated by 45° above and below the in-phase condition, this effect is caused by a change in the form factor of scattering for the different azimuthal directions for different electron energies. This can also explain the half-moon shaped (10) spot shown in Fig. 1: the form factor decreases to zero at the outer side of the ring due to dynamic scattering effects. The uniform intensity distribution around the perimeter of the ring is more evident close to the in-phase condition, where the dynamic form factor, which is only slowly varying with $k_{\parallel}$, stays more and more constant for different azimuthal orientations.

The positions of the ring of the (00) spot in reciprocal space are plotted in Fig. 6 for electron energies ranging from 20 to 160 eV (the k_z axis is compressed by a factor of 2). The x axis is scaled in percent of the Brillouin zone (% BZ), i.e., in fractions of the distance to the next integer-order spot, which corresponds to 100% BZ. The length of the ovals corresponds to the full width at half maxima of the rings; the width describes the intensity of

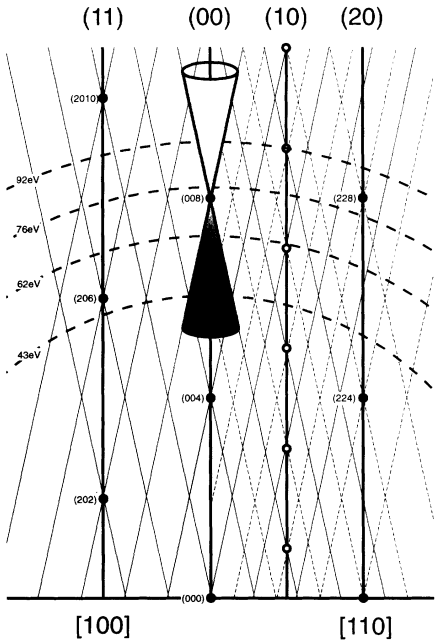

FIG. 4. The facet rods of the 12° cones on the (001) surface in the reciprocal space are plotted for two different azimuths. The in-phase conditions (the Bragg conditions) are plotted by dots and open circles. In the [100] direction [towards the (11) spots] no double periodicity occurs. The two nonequivalent steps in the [110] direction cause an inherent double periodicity (dashed lines) on these facets and thus double that many facet rods. The location of the 2D scans of Figs. 1–3 and the 1D scan of Fig. 7 are shown as dashed circle segments. The diffraction pattern of a 12° cone is in the reciprocal space; the cone is shaped like an ice-cream cone with an aperture angle of 24° (two times 12°). These reciprocal-space cones are opened upwards and downwards and located at any in-phase condition of scattering.

the ring qualitatively. Changing the electron energy all spots move on inclined rods with a tilt angle of $\sim 12°$ corresponding to a [117] or [105] direction, which is the typical behavior of the LEED pattern of a faceted surface. But in this special case all possible azimuthal facets with an inclination angle of $\sim 12°$ occur at the surface. No azimuthal orientation of the facets is favored; the ring shows (apart from the dynamic effects) a uniform intensity distribution. Up to now two possible configurations may exist on the surface: either circular cone-shaped islands or the existence of islands with all possible azimuthal facet orientations. It seems to be more plausible to have only one type of island shape at the surface, even if this is a perfect cone. We will show later in Sec. V that this is indeed the case.

The diffraction pattern of a 12° cone in the reciprocal space is also a cone which, however, is shaped like an ice-cream cone with an aperture of 24° (two times 12°), as shown in Fig. 4. These reciprocal-space cones are opened upwards and downwards and located at any in-phase condition of scattering (open and closed dots in Fig. 4).

The atomic arrangement of the facet depends on their azimuthal orientation. The LEED patterns around the out-of-phase condition for single steps at about 40 eV show four distinct spots in the [110] direction, which show with a [117] orientation also the same facet behavior as the rings (plotted as open ovals in Fig. 6). The explanation is a double periodicity along the tilted direction of the [117] facets as a double step height or a (2×1) reconstruction for this azimuthal orientation. This is an inherent property of this facet because the steps have an alternating geometry referred to as an *A*-type and a *B*-type step in the literature.[16] In contrast the [105] facet [oriented towards the (11) spot] could be built up without an additional periodicity because successive steps in this direction have an identical geometry, thus lacking this extra facet spot. The hut clusters of the Si(001)/Ge system without Sb also consist of [105]-type facets, but reconstruct in a (2×2.5) structure;[11] in our case the Sb on the [105] facets hinders the formation of a reconstruction.

The 12° cones show a vertical layer distance of Ge which is slightly larger than the Ge bulk lattice parameter. Compared with the Ge bulk parameter value of 1.414 Å, the 12° cones have a 1.6% increased layer distance of 1.438 Å, as estimated from the in-phase conditions [the intersections of the facet rods with the (00) rod], which are slightly shifted to lower values. This tetragonal distortion of the 12° cones is caused by the pseudomorphic growth with the lateral lattice positions of the Ge atoms determined by the Si substrate.

This is also confirmed by a measurement of the positions of the $(\bar{1}0)$, (00), and (10) spots of the 12° cone-shaped surface showing exactly the same spot positions

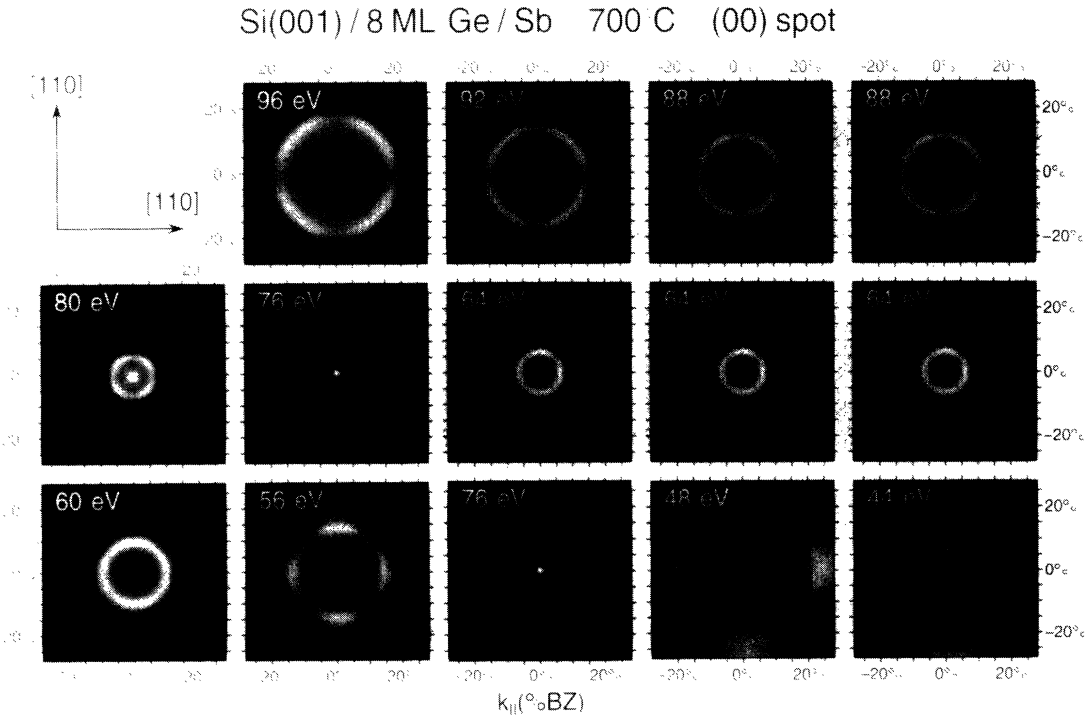

FIG. 5. The diameter of the ring around the (00) spot depends on the electron energy as shown in this series of 2D scans. The in-phase condition at 72 eV is clearly seen in the presence of the sharp central spot. The intensity of the ring is fourfold modulated by dynamic effects: at high energies weak maxima occur in the [100] directions, at low energies in the [110] directions. The four distinct intensity peaks at 48 and 44 eV are caused by the [117] facet, which has a double periodicity. Those peaks coalesce at the out-of-phase condition for single steps at 39 eV.

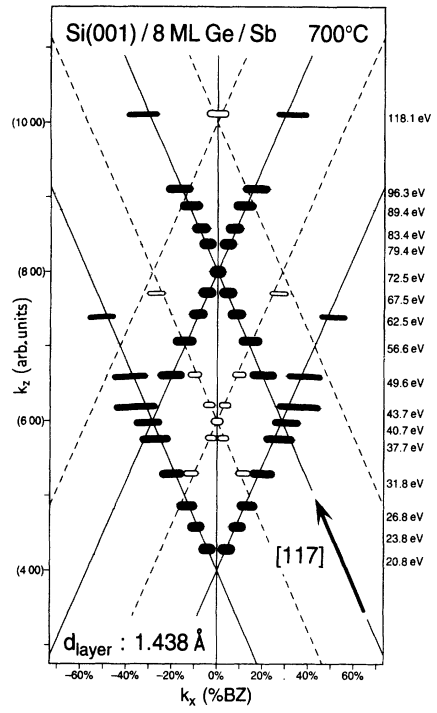

FIG. 6. The position of the intensity ring around the (00) spot is plotted as ovals in reciprocal space as a function of k_z, indicated with the Bragg conditions. The length of the ovals corresponds to the width of the rings, the width roughly to the intensity of the rings. Open ovals denote the [117] facet spots which only occur in the [110] directions. The spots move on rods, which are inclined by $\sim 12°$, indicating a facet behavior. From the in-phase conditions, which are determined with very high accuracy from the intersections of the facet rods with the (00) rod, a layer distance of 1.438 Å is estimated, which is about 1.6% larger than the Ge bulk value.

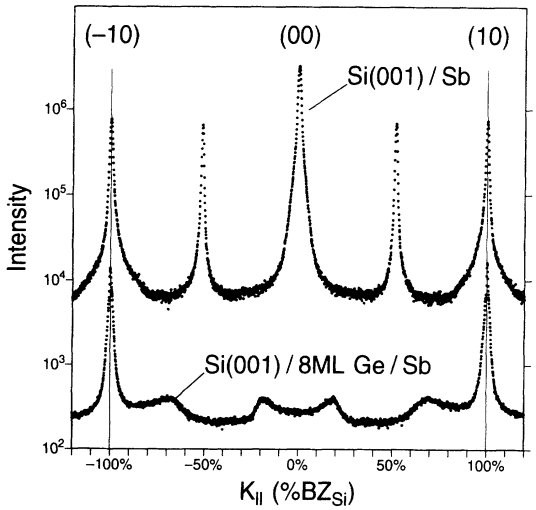

FIG. 7. The 12° cones are pseudomorphic and show the same lateral lattice constant as the Si substrate as measured with identical positions of the ($\bar{1}0$) and (10) spots of the bare surface and the 12° cone covered surface. The in-phase condition for the (10) spots with an electron energy of 94 eV has been chosen as a scattering condition, producing the sharp spots necessary for the comparison.

(accuracy ±0.003 Å) compared with a Si surface (Fig. 7). The in-phase condition for the (10) spots with an electron energy of 94 eV has been chosen as a scattering condition, as also sketched in Fig. 4). The intensity ring of the (00) spot can be seen in the lower curve at ±20% BZ. These data additionally confirm that the 12° cones are still pseudomorphic without any strain-relieving defect generated up to that coverage.

The whole surface is covered by 12° cones as seen in the nearly complete lack of intensity at the (00) spot position for scattering conditions other than the in-phase condition (see Figs. 2, 3, and 5). A large flat surface area would produce intensity confined around $K_{||}=0$. This area has been estimated by applying a very simple model of incoherent scattering to the LEED spot profiles. It is assumed that the relative intensity scattered into a reciprocal-space area is proportional the area on the sur-

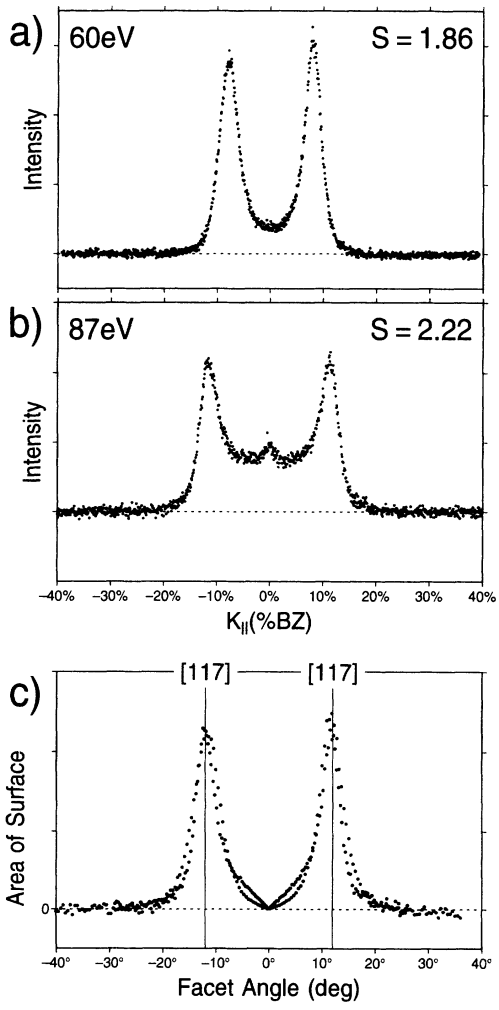

FIG. 8. (a) and (b) Spot profiles of the ring at two different energies show an increased intensity inside the ring. This intensity may be caused by a rounded top instead of a sharp peak of the islands or other flat areas of the surface. (c) The portion of the area with a distinct inclination angle is evaluated in a simple model of incoherent scattering. There are nearly no flat areas, since the intensity of the linear scans has to be weighted linearly because of the isotropic intensity distribution of the ring.

face covered with that distinct facet orientation. Thus the intensity portion located around $K_{\parallel}=0$ is caused by flat areas of the surface. Two different spot profiles recorded at 60 and 87 eV are plotted in Figs. 8(a) and 8(b). The electron energies correspond to different scattering phases S, thus producing different diameters of the rings; refer also to Fig. 6. The intensity inside the ring seems to be quite high and also different for both profiles. But the evaluation has to be carried out for the whole two-dimensional profile, thus multiplying the one-dimensional scans of Fig. 8 by $K_{\parallel}$ and therefore strongly reducing the weight of intensity on the inside of the ring. The resulting area of the surface as a function of the tilt angle of the facets is shown in Fig. 8(c). The facet tilt angles are very sharply peaked around the [117] orientation.

The low intensity observed in broad (2×1) spots at some energies may be caused by small areas, which are more or less flat, as expected between the 12° cones or on top of the 12° cones (from general energetic reasons rounded tops of the 12° cones are favored due to the high temperatures[19]).

The size of the 12° cones could also be estimated from the LEED analysis. A finite-size effect in the diffraction has to be expected for the cones if they are smaller than the transfer width of the instrument ($\sim$1000 Å). The width of the intensity ring depends on the scattering phase S, which, on the other hand, linearly corresponds to the diameter of the ring (see Fig. 9). At the out-of-phase condition the size distribution of the single terrace of the facets is observed in the width of the ring (the diameter of the ring, however, is determined by the facet angle). Changing the scattering condition more and more towards the in-phase condition reduces the width of the intensity distribution of the ring due to the larger lateral distances necessary to cause a phase shift of π. At the in-phase condition the spot profile is determined by the distance between the 12° cones. Unfortunately the broadened part of the spot disappears for this condition, since all atoms scatter constructively without any phase difference. However, the distance distribution of the 12° cones still determines the spot profile for scattering phases very close to the in-phase condition. The range of validity depends on the maximum height difference Δh of the structures and is roughly given by $S\pm\Delta S$ with $\pm\Delta S=1/\Delta h$ and S equal to the integer number given by the in-phase condition.

The width of the ring decreases linearly to lower values with decreasing diameter of the ring as shown in Fig. 9, but shows an asymptotic behavior towards a constant

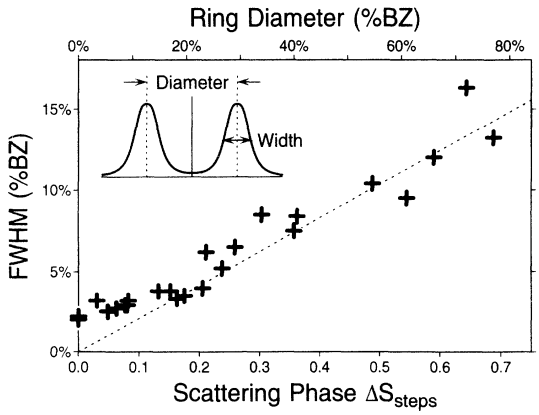

FIG. 9. The full width at half maximum of the rings increases linearly with the diameter of the ring or the scattering phase S (both parameters are coupled by the inclined facet rods). From the asymptotic behavior of the width towards a constant value of 2.2% the BZ close to the in-phase condition is estimated as a finite-size effect of 12° cones of $\sim$300–400 Å.

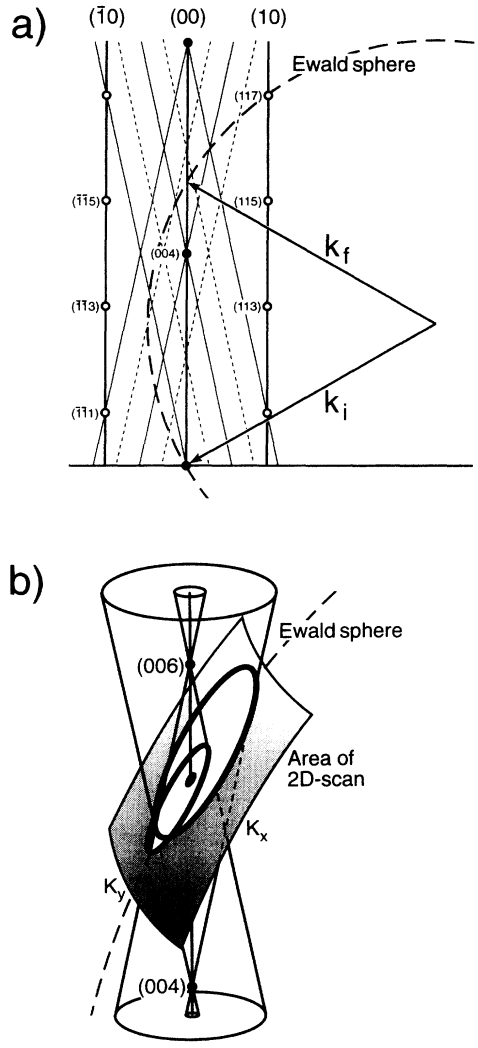

FIG. 10. Plot of the reciprocal space with the Ewald sphere for the geometry used with the external electron gun. Due to the 30° incident angle the LEED pattern is distorted by an extension of roughly a factor of 2 in the k_x direction. Additionally complicating is the dependence of k_z or the scattering phase S on the k_x component of the scattering vector. This leads to a strong distortion of the rings to deformed ellipses since the LEED pattern of the 12° cones strongly depends on the phase S. The result is sketched in the lower part of the figure: two intersecting ellipses form, one from the upward opened cone and the other from the downward opened cone, in the reciprocal space.

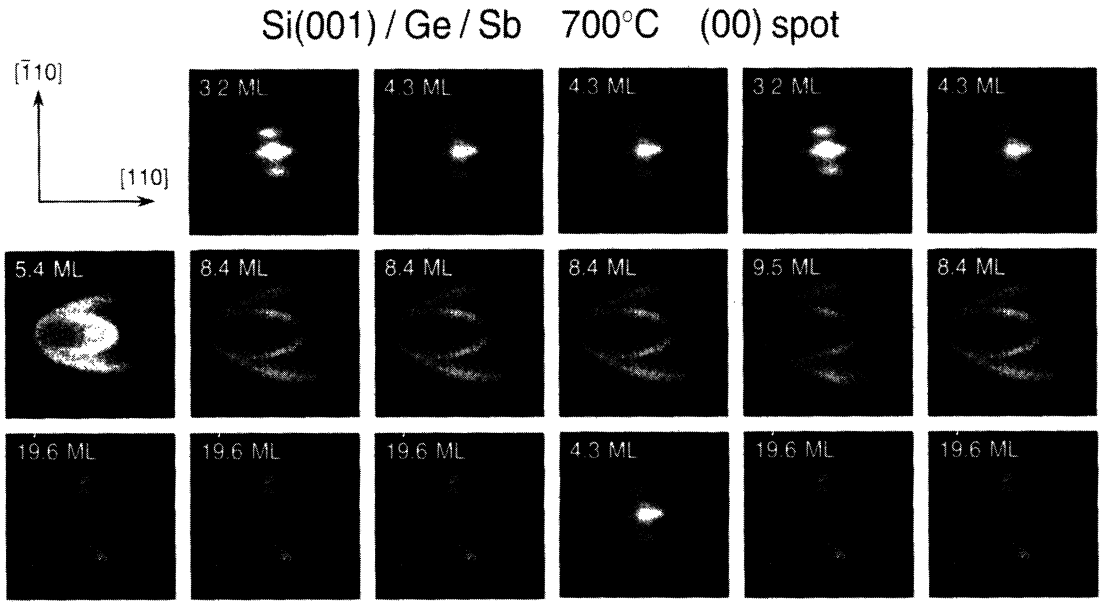

FIG. 11. A series of 2D scans reveals the formation of the 12° cones during the deposition. The LEED pattern is distorted due to the external gun geometry, as already shown in Fig. 10. The cones appear at ~5 ML and are visible up to ~12 ML of Ge. The size of the ellipses is increasing with coverage, indicating an increase of the facet tilt angle.

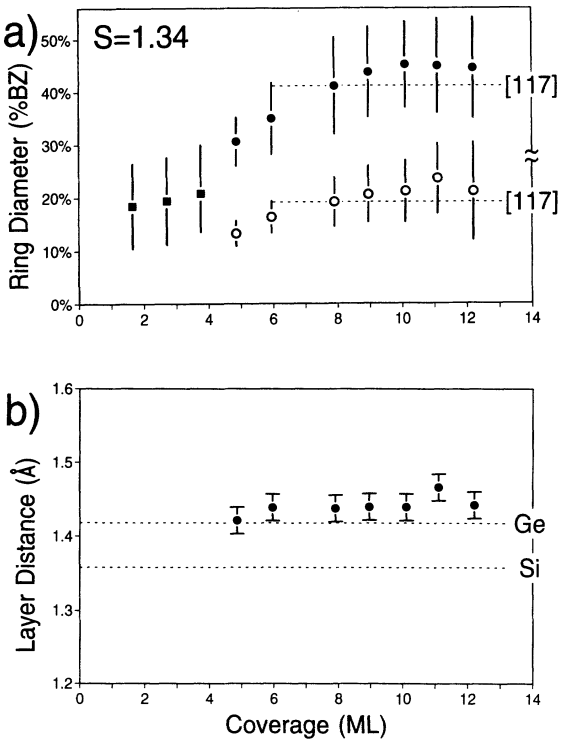

FIG. 12. (a) The diameter of the ring (open and closed circles) and the facets (squares) increases with the coverage indicating an increase of the tilt angle of the 12° cones with a saturation towards a [116] facet. At 8 ML an angle of ~12° corresponding to a [117] facet is observed. (b) The layer distance in the 12° cones during growth is derived as mentioned in the text and in Fig. 13. The Ge 12° cones deform due to a tetragonal distortion caused by the pseudomorphic growth.

value of 2.2% BZ. This behavior reflects the finite size of the 12° cones. An average distance of the 12° cones of about 300–400 Å is estimated. This is a reasonable value since an average diameter of 330 Å results by assuming the whole surface covered with cones which have a tilt angle of 12° and are built up by a total coverage of 8 ML of Ge.

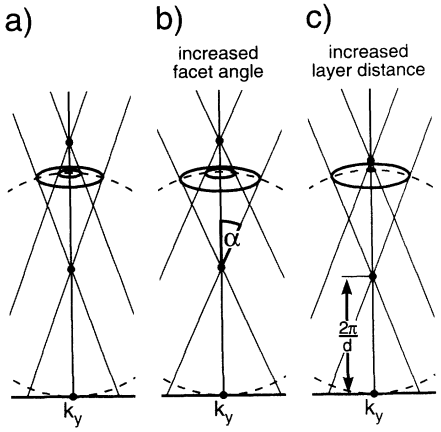

FIG. 13. The presence of two rings in the LEED pattern allows the determination of the facet tilt angle as well as the layer distance as shown in these diagrams of the reciprocal space. (a) Unchanged geometry. (b) An increase of the facet tilt angle results in a larger angle of the facet rods in reciprocal space. The in-phase conditions are not affected. Both rings change their diameter by the same factor. (c) An increase of the layer distance changes the location of the in-phase conditions. Since one of the cones in reciprocal space is opened upwards and the other downwards, the first increases its diameter, whereas the second reduces its diameter.

IV. LEED RESULTS DURING DEPOSITION

The dynamic of the formation of the 12° cones has been studied during Ge deposition at 700 °C with SPA-LEED using the external electron gun. The LEED pattern is distorted due to the incidence angle of 30°. This situation is sketched in Fig. 10(a). Additionally complicating is the dependence of the scattering phase S on the K_x component of the scattering vector, causing a strong distortion of the rings towards deformed ellipses since the LEED pattern results from the intersection of the cones in reciprocal space with the Ewald sphere [Fig. 10(b)]. Two intersecting distorted ellipses are observed in a series of 2D scans of the (00) spot for increasing coverage shown in Fig. 11 and correspond to two reciprocal-space cones, one of them opened upwards, the other downwards. The measurement has been performed at an electron energy of 140 eV corresponding to a scattering phase of $S=1.34$.

Distinct facet spots in the [110] azimuthal direction occur up to a coverage of 5 ML of Ge. The tilt angle of the facets increases with coverage. The surface still has flat areas indicated by the intense central spot. Beyond 5 ML the rings are clearly visible, the remaining central spot vanishes at a coverage of 6 ML. The rings become more faint above 10 ML with a pronounced intensity peak in the [110] direction indicating again facets at the surface.

The distance between the facet spots and the diameter of the ring increase with coverage. This behavior has been monitored in a series of linear scans in the K_y direction. The positions of facets (squares) and rings (dots) as a function of coverage are plotted in Fig. 12(a). The tilt angle of the facets increases with coverage and saturates at a little bit steeper facet than a [117] orientation, which is marked by the dashed lines. The width of the rings (see Fig. 9) is plotted as solid lines crossing the dots and squares. The more or less linear increase of the facet angle points to a growth with constant island size and a linear increase of the height of the 12° cones. A constant facet angle during growth would require an increasing size of the islands starting with very small islands. Such a behavior can be seen for higher coverages, where the facet angle stays constant, indicating the growth of larger islands, which is probably accompanied by the generation of strain-relieving defects.

The Ge layer distance in the 12° cones can also be estimated during growth. A change of tilt angle increases the diameter of both rings by the same factor without changing the position of the in-phase conditions, whereas an increase of the layer distance compresses the cones in reciprocal space to lower K_z values as sketched in Fig. 13. Thus the reciprocal-space cone opened upwards with the in-phase condition at $S=1.0$ increases in diameter (this is the larger ring in Fig. 11), whereas the reciprocal-space cone opened downwards (in-phase condition at $S=1.5$, the smaller ring in Fig. 11) decreases in diameter. The change of the layer constant is calculated as the ratio of both diameters, thus eliminating the influence of change in tilt angle. The values for the layer distance during growth are shown in Fig. 12(b). The dashed lines show the values for the Si and Ge bulk parameters. The accuracy of about $\pm 2\%$ of these data is sufficient to observe indeed an increase in the Ge layer distance in the

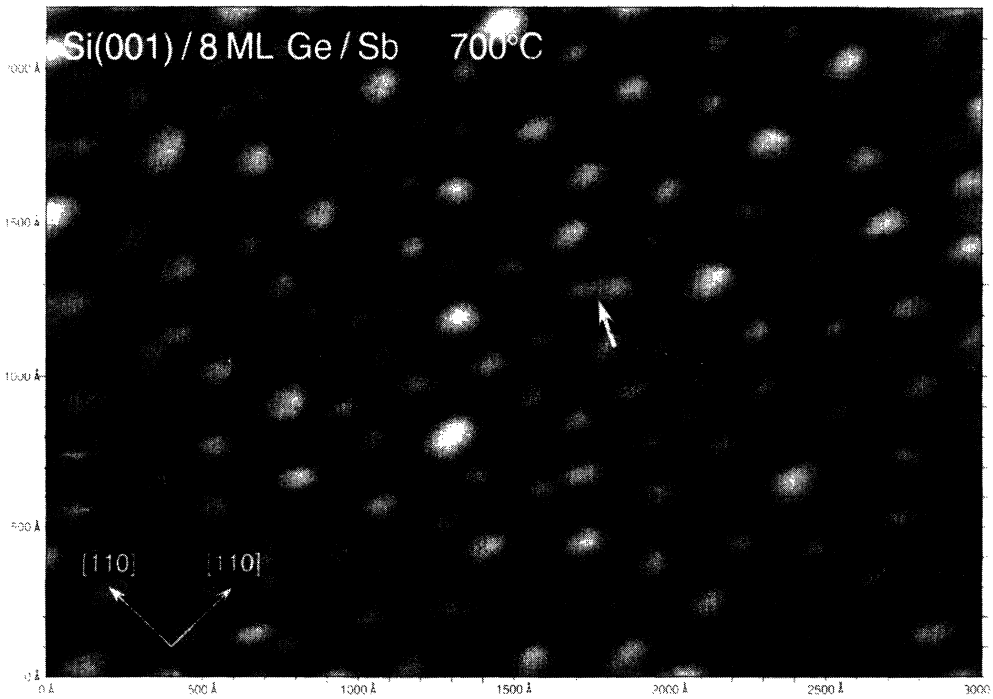

FIG. 14. STM image with a size of 3000×2200 Å after deposition of 8 ML of Ge on Si(001) with Sb as surfactant at 700 °C. The 12° cones cover the whole surface without any empty places. Areas between larger 12° cones are filled by very small islands.

12° cones which is consistent with the estimation from the measurement shown in Fig. 6.

V. STM RESULTS

A STM image of the Si(001) surface covered with 8 ML of Ge grown at 700 °C with Sb acting as a surfactant is shown in Fig. 14. The whole surface is covered by 12° cones. No flat areas are visible, not even between the cones; those spaces are filled up with smaller islands. The majority of the surface is covered with 12° cones having a typical size of ~300 Å. No islands larger than 400 Å are present. There is only one island (arrow) which seems to have been coalesced from two 12° cones, which may be accompanied by the formation of a strain-relieving defect.

The island-distance or -size distribution has been evaluated in two different ways. First the size of any cone apparent in Fig. 14 has been estimated. Those data are shown in Fig. 15(c) as that portion of the surface covered with 12° cones of a given diameter. The size distribution is strongly peaked for 12° cones with a diameter of about 80 unit cells, i.e., 300 Å. This indicates that all 12° cones have nearly the same size, therefore reducing the strain in the film to the smallest possible value without generation of defects. Larger cones are unfavorable since they accumulate more strain energy; smaller cones are strain relieved to a higher degree. This, however, will only happen under equilibrium conditions during growth of the film. The Ge atoms must be mobile until they find the most favorable lattice site; they even must be able to detach again from a lattice site which they already had occupied. This, however, is usually prohibited by a surfactant at lower temperatures: an atom is no longer mobile and is trapped as soon as it is bonded in a lattice site. This selective change of the kinetics is just the way a surfactant forces layer-by-layer growth.[12]

The second way of determining the island-distance distribution (which is nearly the same as the island-size distribution, since the 12° cones are covering the whole surface and the distribution is quite sharp) is done via the Fourier transform of the STM image. The square modulus results in the intensity distribution expected for the broadening of the LEED pattern at or very close to the in-phase condition of scattering.[20] Assuming the simple model of incoherent scattering the intensity in a reciprocal-space unit can be transformed into the area of the surface covered with 12° cones of that diameter.

The two-dimensional Fourier transform of the STM image is shown in Fig. 15(a). Now the ring-shaped intensity distribution is caused by the distance distribution of the 12° cones and not by the shape of the 12° cones, which is not detectable at the in-phase condition of scattering (refer also to the explanation of Fig. 9). The irregular structure along the ring perimeter is probably an artifact of the very small area transformed (only ~200 cones have been in the statistics). The intensity dips toward the [010] directions, however, may be a hint for preferred positions of neighbored 12° cones. The diameter of 2.25% BZ of the ring corresponds very well with the width of

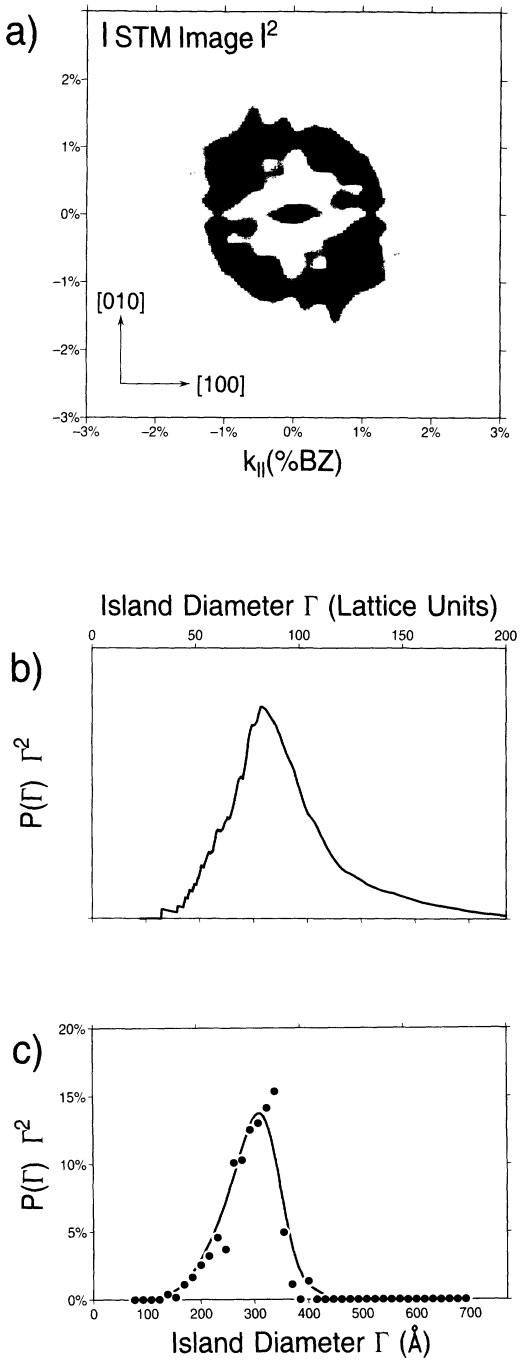

FIG. 15. The island-size and island-distance distribution is derived. (a) The square of the Fourier transform of the STM image shown in Fig. 14 reflects the 12° cone distance distribution and is identical to a LEED pattern close to the in-phase condition. The distribution shows maxima in the [100] directions, which is a hint for the preferred next-neighbor cone site. (b) The resulting isotropic distance distribution shows a very sharp maximum at a length of ~80 atoms, i.e., 300 Å. (c) The island-size distribution has been determined by estimating the size of any 12° cone visible in Fig. 14 and shows also very sharp maxima with a complete lack of 12° cones larger than 400 Å. These sharp-peaked distributions are a result of the equilibrium formation process of the 12° cones.

the ring measured with SPA-LEED at the in-phase condition (see Fig. 9). The resulting island distance distribution [Fig. 15(b)] after averaging over all azimuth angles shows also a maximum at ~300 Å, as already seen in Fig. 15(c).

A higher magnification of the surface reveals the atomic structure of the 12° cones as shown in Fig. 16 in a 3D view with an exaggerated height scale. Essentially two different facets could be distinguished. The [117]-type facets with a regular pattern of atomic steps has a quite smooth face. The [105]-type facet, which in the figure is parallel to the border of the image, is irregularly shaped with a high number of kinks.

The top of the 12° cone is rounded and not sharply peaked. A convolution effect with the shape of the tip in the STM is ruled out since the arrangement of the atoms on top of the 12° cones is different from cone to cone. The rounded top of the 12° cones is more likely caused by the non-zero-temperature effect,[19] allowing facets other than those with the lowest energy.

VI. SEM RESULTS

We have also performed scanning electron microscopy (SEM) measurements in order to ensure that large 3D clusters have not formed. It is difficult to detect those with LEED or STM, since they may cover only a very small portion of the surface, but nevertheless may contain a large fraction of the Ge coverage. The SEM, which we have used, could resolve Ge islands with a minimum size of 1000 Å.

The sample grown with surfactant shows no visible structure of an area of $\sim 10 \times 10$ μm except a small dirt particle used to focus [Fig. 17(a)]. Thus all Ge deposited is confined in the small pseudomorphic 12° cones without formation of any large 3D clusters.

However, 3D clusters form during growth without a surfactant and are visible in the SEM image [Fig. 17(b)] of 8 ML of Ge grown at a temperature of 700 °C. Both images have the same magnification. The 3D clusters have two different sizes of ~4000 and ~1000 Å.

VII. KINETICALLY LIMITED GROWTH AT LOWER TEMPERATURES

Growing the films at temperatures lower than 700 °C results in a qualitatively different surface morphology. The LEED pattern at the out-of-phase condition of 8 ML Ge films has a fourfold symmetry as seen in Fig. 18 for all temperatures from 600 °C down to 400 °C. The surface roughens laterally in the form of short terraces, as seen in the strong broadening observable at all temperatures. The spot profile becomes more structured with increasing temperature up to clearly visible extra spots indicating a (1×8) periodicity on the surface. The spot profiles at the out-of-phase condition are plotted in Fig. 19 in a logarithmic intensity scale and show roughly the same width, only changing their shape with temperature. The profile at 400 °C is described by a Lorentzian function[21] (with a geometrical terrace distribution) with a width of 25% BZ, resulting in an average terrace length of only 2.6 ± 0.2 unit cells, i.e., 10 Å.

For all growth temperatures the surfaces of the films show a high vertical roughness as measured by the depen-

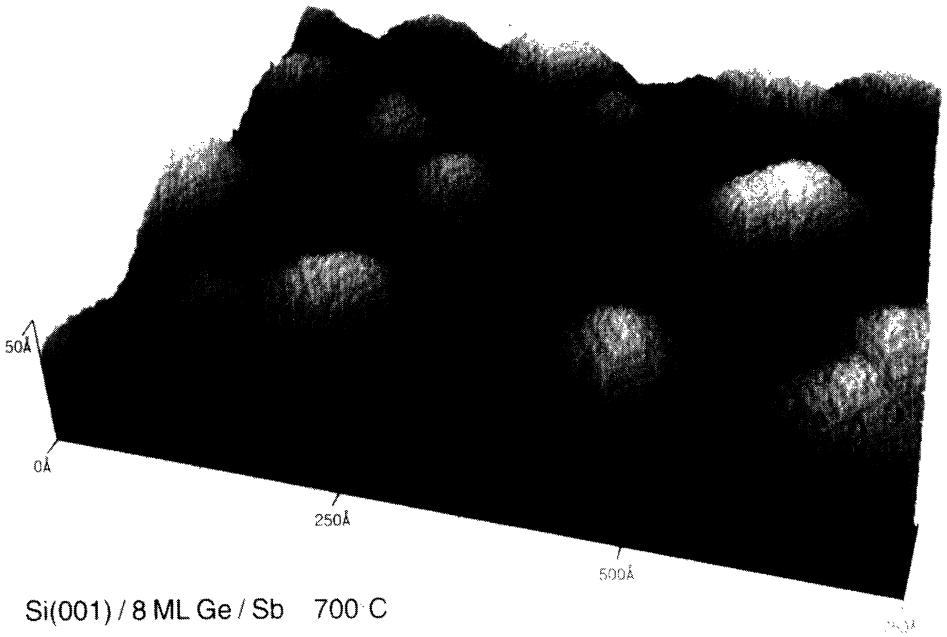

FIG. 16. The 12° cones are seen with atomic resolution in this perspective STM image with a size of 1000×700 Å (the height scale is exaggerated by a factor 2). The [105] facet (parallel to the border of the image) shows an unordered structure, whereas on the [117] facet even the double periodicity is observable. The 12° cones are not peaked but have a rounded top, reconstructed in a (2×1) structure.

dence of the spot profile on energy. In Fig. 20 the relative central spike intensity, the $G(S)$ curve [normalized to the total intensity of the (00) spot, thus eliminating the dynamic form factor, resulting in the structure factor $G(S)$ of kinematic scattering], is plotted, which results from the constructive interference between the layers. It is a sensitive measure of the vertical roughness.[22] The values are plotted as a function of the scattering phase S (or the electron energy). The $G(S)$ curve is peaked at the Bragg conditions for the Ge film, where $S=1$ corresponds to the (004) reflex in x-ray scattering and $S=2$ to the (008) reflex. The very sharp spots with all intensity confined in the central spike reflect the high quality of the epitaxial growth of the Ge down to 320 °C. The strong decrease of the $G(S)$ curve around the Bragg conditions with a full width at half maximum of the curves of $\Delta S=0.25-0.30$ reflects a rms value of the roughness[23] of $\Delta=1.3-1.1$ atomic layers (one layer $=1.47$ Å), thus a

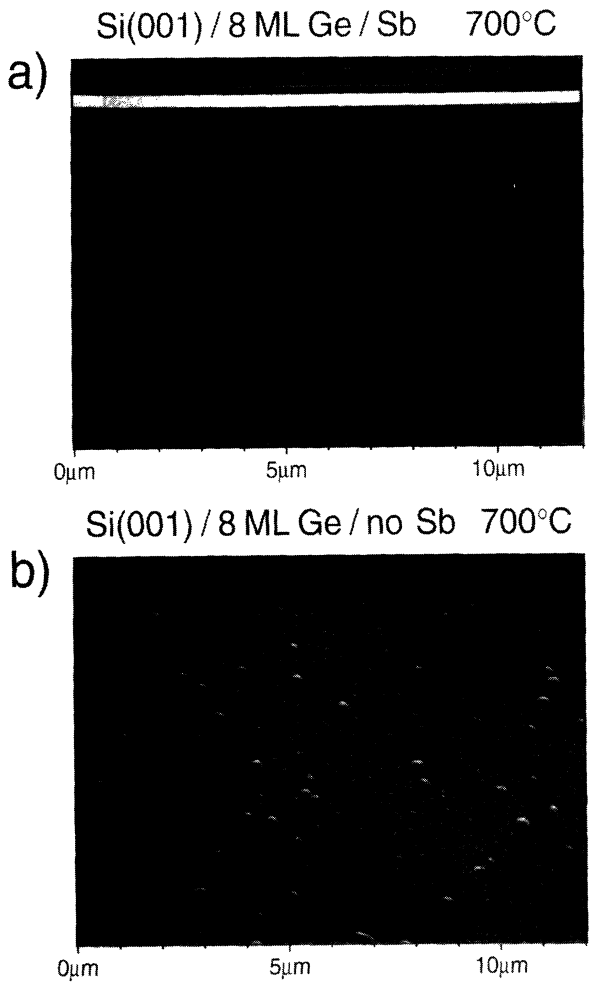

FIG. 17. (a) Using Sb as a surfactant during the deposition of Ge suppresses formation of large 3D clusters as shown in the SEM image of $\sim 10\times 10$ μm size. The 12° cones are not visible due to the poor resolution of the instrument used. (b) Growth without surfactant results in the formation of a high number of 3D clusters with two different sizes of ~ 4000 and ~ 1000 Å diameter.

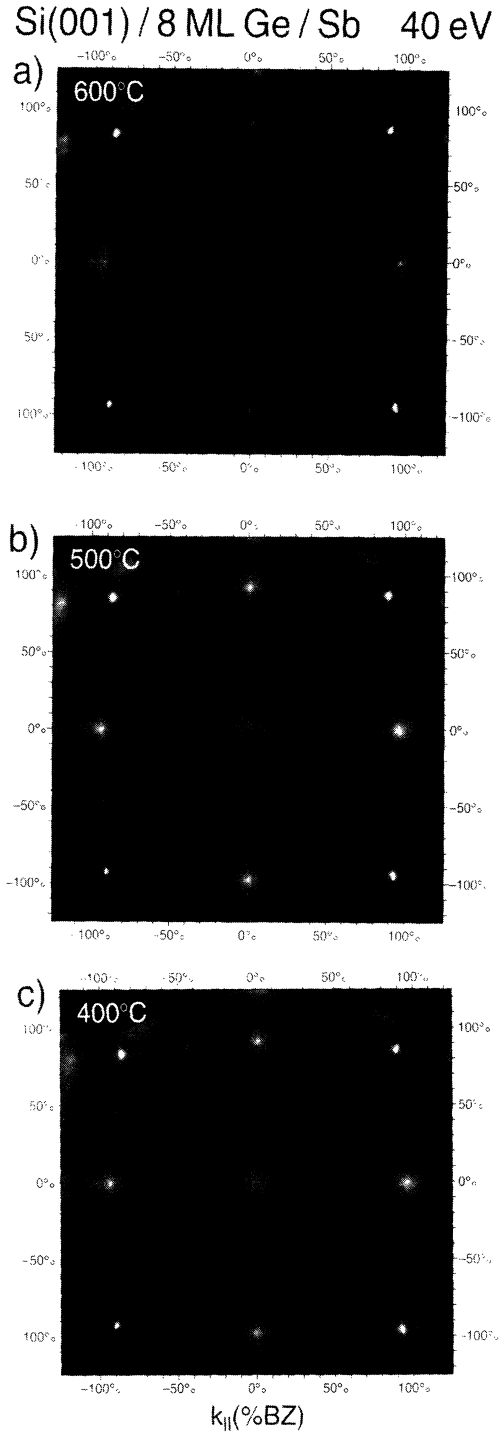

FIG. 18. Growth of 8 ML of Ge at lower temperatures results in quite different behavior. The sharp (11) spots indicate for all temperatures perfect epitaxial growth [41 eV is the in-phase condition of the (11) spots but the out-of-phase condition for the (00) spot]. The strong broadening of the (00) spot at all temperatures reflects the same lateral strong roughness of the Ge film. (a) At 600 °C growth temperature the LEED pattern shows a (8×2) reconstruction, as an ordered-surface morphology. (b) At 500 °C the LEED pattern still has some structure resembling the (8×2) seen at 600 °C. (c) At 400 °C and lower the broadening is featureless and could be described by a Lorentzian function.

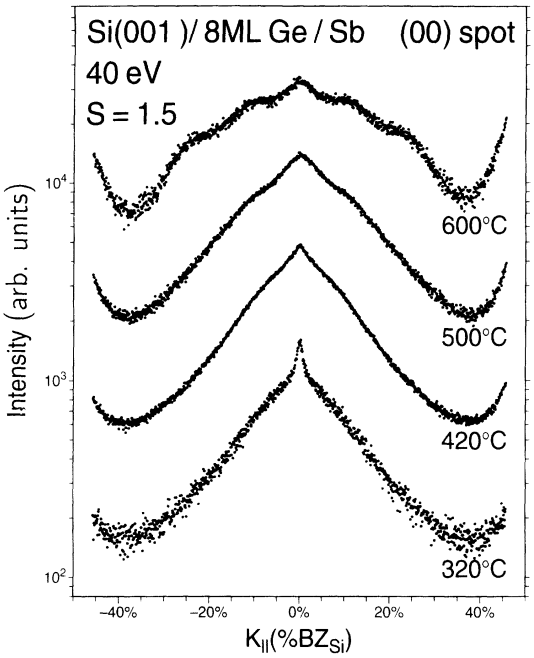

FIG. 19. Linear scans through the (00) spot at the out-of-phase condition show the increase of order with increasing temperature. The spot profile changes from a Lorentzian to the (2×8) structure. The width of the profiles, however, stays nearly constant over that large temperature range. Thus the roughness is not formed by kinetics but as a strain relief mechanism due to the lattice mismatch of 4.2% between Si and Ge.

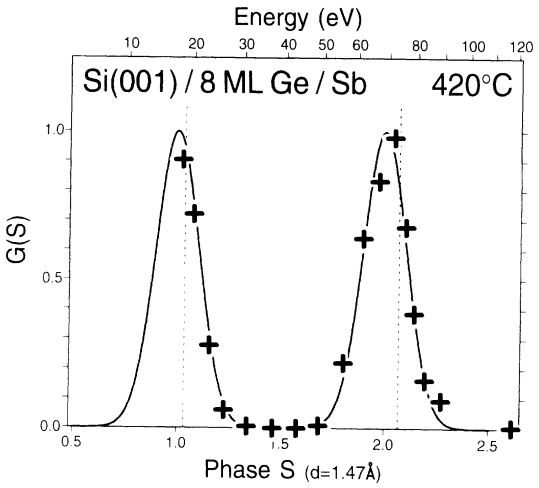

FIG. 20. The vertical roughness is determined from the ratio of central spike to total intensity in the (00) spot, i.e., the $G(S)$ curve. At the in-phase conditions, here at 16 and 68 eV, only the central spike remains since all unit cells scatter in phase (Bragg condition). The strong decrease of the $G(S)$ value for small deviations from the in-phase condition reflects the large microroughness of the film. A rms value of the roughness of $\Delta = 1.1$ is derived.

quite rough surface. This rough surface is not caused by the kinetics of growth since the value Δ does not depend on the temperature but stays nearly constant from 320 °C up to 600 °C.[19] The driving force is the strain relief by the introduction of microroughness for the non-lattice-matching materials.

The tetragonal deformation of the pseudomorphic Ge films is measured by the slight shift of the $G(S)$ curve to lower energies compared with the Bragg conditions expected for relaxed Ge bulk materials (dashed lines). This extension of the layer distance (Ge bulk: 1.41 Å) is on the order of (0.055±0.02) Å for all 8 ML of Ge films.

Also the STM images reveal the quite different surface morphology for the temperature regime below 700 °C. In Fig. 21(b) [Si(001)/8 ML Ge/Sb at 600 °C] the nature of the (1×8) periodicity seen in LEED becomes clear: the Ge forms trenches consisting of missing dimers on top of a still rough film in order to relieve strain.[24] The remaining Ge terraces have a typical size of about 8×8 atoms, thus causing the extra spots in LEED. Due to the irregularity in the size and arrangement of the 8×8 patches, the $\frac{2}{8}$ spot is much broader than the $\frac{1}{8}$ spot [see also Fig.

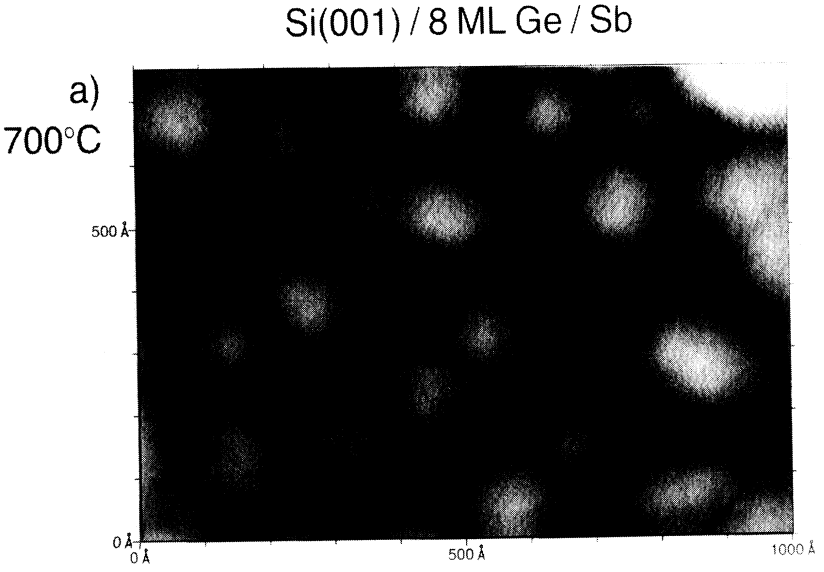

FIG. 21. The change from growth under equilibrium conditions to a growth under kinetic limitations is seen in this series of STM images for different growth temperatures. (a) At 700 °C growth temperature the STM shows the 12° cones. (b) At 600 °C the (2×8) becomes apparent in the STM. Even terraces on the same level are separated by one-atom-wide trenches in order to relieve strain. (c) At 530 °C the Ge film is quite rough and composed of small Ge terraces forming Ge islands with a size of ~400 Å.

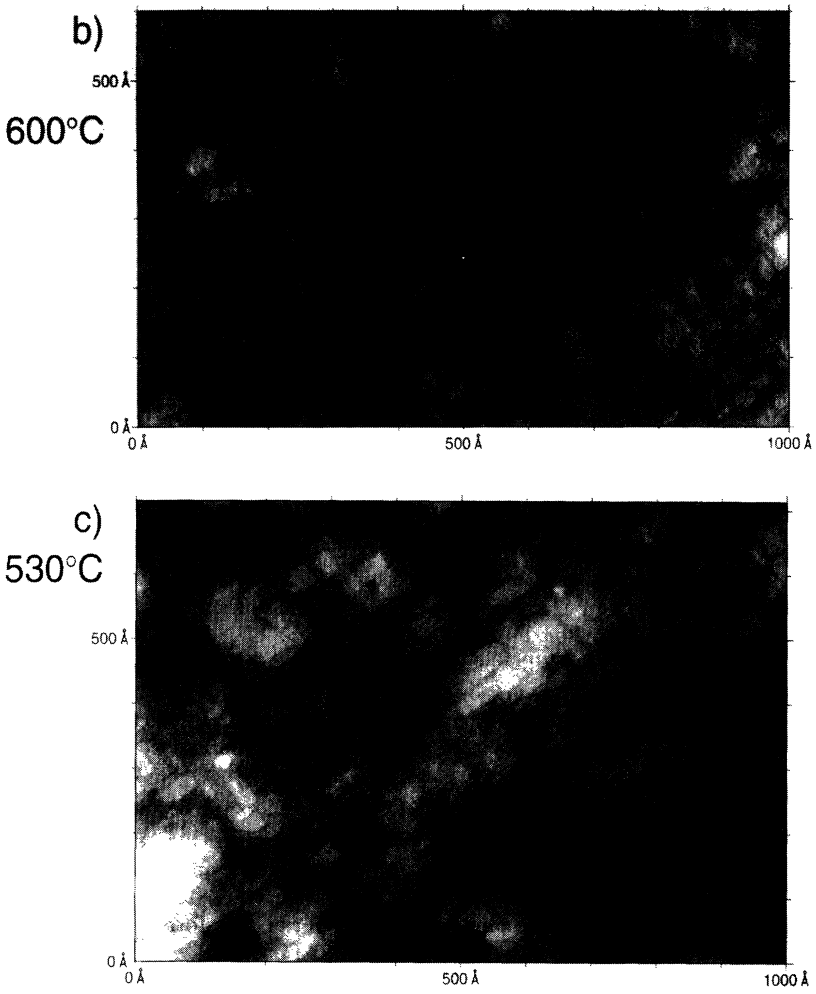

FIG. 21. (*Continued*).

18(a)].

The 8 ML Ge film grown at 530 °C [Fig. 21(c)] no longer relieves strain by the introduction of missing dimers. Terraces on one level—even if they are quite large—have a single domain (2×1) surface. The film as observed by the STM is again very rough with a variety of terrace sizes, but an average size of ~10–20 Å, which is consistent with the LEED results. The terraces have an anisotropic shape, as is often found for the (001) surface of semiconductors.

The overall island size (an island is defined as the larger structures built up by terraces on different levels and separated by the very deep trenches down to the Stranski-Krastanov layer or to the Si substrate) is similar to the size of the 12° cones. This shows that the islands grown in the kinetically limited regime also have a typical size which is given by the lattice mismatch as long as the growth is in the pseudomorphic regime and no dislocations have been generated.[19,25]

VIII. CONCLUSIONS

We have reported the formation of epitaxially strained Ge islands with a circular, flat cone-shaped form (12° cones) after deposition of 8 ML of Ge at 700 °C using Sb as a surfactant. They are grown pseudomorphically with the Si lattice constant. The size distribution of the 12° cones is sharply peaked at 300 Å, indicating an equilibrium process of the formation. This is also supported by a reversible change of the island depending on the Sb coverage.[15]

Because the Ge diffusion is no longer hindered, the Sb-covered 12° cones are energetically favored compared to the formation of strain-relieving defects, which are usually already formed without a surfactant at this coverage of 8 ML of Ge and lead to the formation of 3D clusters. The reduction of the surface free energy by saturation of dangling bonds seems to be larger for the facets than for the flat (001) surface and balances the strain energy necessary for the pseudomorphic growth of the 12° cones. This delicate balance breaks as soon as the coverage exceeds ~10–12 ML of Ge, thus accumulating enough strain to generate defects. The process is not a true equilibrium process because it is not independent of the history of the film preparation: it is not possible to dissolve large 3D Ge clusters which form during growth without Sb and are strain relieved by defects, just by applying Sb after growth; they keep stable.

Growth under kinetic limitations by the surfactant creates qualitative different Ge films. Those films are also microrough in order to relieve strain by a lateral partial

relaxation of the Ge atoms towards their own bulk lattice parameter. But the islands formed by this process do not show the regular form and size of the 12° cones but have a more or less unordered shape depending on the growth temperature.

ACKNOWLEDGMENTS

Financial support by the Deutsche Forschungsgemeinschaft is gratefully acknowledged. We acknowledge useful discussions with J. Wollschläger and T. Schmidt.

*Electronic address: michael.horn-von-hoegen @CDC2.festkoerper.physik.uni-hannover.d400.de

[1]M. Copel, M. C. Reuter, E. Kaxiras, and R. M. Tromp, Phys. Rev. Lett. **63**, 632 (1989).

[2]M. Horn-von Hoegen, F. L. LeGoues, M. Copel, M. C. Reuter, and R. M. Tromp, Phys. Rev. Lett. **67**, 1130 (1991).

[3]H. A. van der Vegt, H. M. van Pinxteren, M. Lohmeier, and E. Vlieg, Phys. Rev. Lett. **68**, 3335 (1992).

[4]T. P. Pearsall, J. M. Vandenberg, R. Hull, and J. M. Bonar, Phys. Rev. Lett. **63**, 2104 (1989).

[5]J. N. Burghartz *et al.*, IEDM 1990, p. 297; A. Gruhle, H. Kibbel, U. Erben, and E. Kasper, EL 1993, p. 415; J. N. Burghartz, J. H. Comfort, G. L. Patton, J. D. Cressler, B. S. Meyerson, J. M. C. Stork, J. Y.-C. Sun, G. Scilla, J. Warnock, B. J. Ginsberg, K. Jenkins, K.-Y. Toh, D. L. Harame, and S. R. Mader, IEDM 1990, p. 297.

[6]U. Köhler, O. Jusko, G. Pietsch, B. Müller, and M. Henzler, Surf. Sci. **248**, 321 (1991).

[7]G. Meyer, B. Voigtländer, and N. M. Amer, Surf. Sci. Lett. **274**, L541 (1992).

[8]M. Horn-von Hoegen, M. Pook, A. Al-Falou, B. H. Müller, and M. Henzler, Surf. Sci. **284**, 54 (1993).

[9]A. Al-Falou and M. Horn-von Hoegen (unpublished).

[10]O. Jusko, U. Köhler, G. J. Pietsch, B. Müller, and M. Henzler, Appl. Phys. A **54**, 265 (1992).

[11]Y-.W. Mo, D. E. Savage, B. S. Swartzentruber, and M. G. Lagally, Phys. Rev. Lett. **65**, 1020 (1990).

[12]The mobility of an adatom is affected little, but an atom, which is bonded to a step or kink site is trapped, since it is not only bonded to the substrate, but additionally to the surfactant, thus strongly hindered to detach again from that position. This desorption is responsible for the creation of the large 3D clusters usually found in the heteroepitaxial growth.

[13]U. Scheithauer, G. Meyer, and M. Henzler, Surf. Sci. **178**, 441 (1987).

[14]M. Horn-von Hoegen, J. Falta, and M. Henzler, Thin Solid Films **183**, 213 (1989).

[15]M. Horn-von Hoegen, B. H. Müller, A. Al-Falou and M. Henzler, Phys. Rev. Lett. **71**, 3170 (1993).

[16]D. J. Chadi, Phys. Rev. Lett. **59**, 1692 (1987).

[17]Because the translation vector for crossing an *A*-type and *B*-type step are different, no reciprocal vector exists for the (10) rod to satisfy a complete destructive interference for both step geometries. Either the *A*-type step has an out-of-phase condition and the *B*-type step an in-phase condition or the other way around. In the [100] directions alternating steps have the same geometry and therefore a reciprocal vector exists for the complete destructive interference for all steps.

[18]For a stepped surface this is valid with all atoms on exact lattice sites. For all other cases (atoms on nonlattice sites such as, for example, the elastic deformation surrounding a dislocation) the point symmetry of the diffraction pattern applies only for the (000) Bragg condition.

[19]E. D. Wiliams and N. C. Bartelt, Ultramicroscopy **31**, 36 (1989).

[20]The LEED pattern close to the in-phase condition can be calculated using the Taylor series of the exponential function $I(\mathbf{k})=|\int d\mathbf{x}\, e^{i\mathbf{k}\cdot\mathbf{x}}e^{-i2\pi\Delta S h(\mathbf{x})}|^2 \simeq I_{\text{spike}}\delta(\mathbf{k}) +4\pi^2\Delta S^2|\int d\mathbf{x}\, e^{i\mathbf{k}\cdot\mathbf{x}}h(\mathbf{x})|^2$, with ΔS as the deviation from the exact in-phase condition. The first term is the delta function caused by the constructive interference and the second term is the broadened part of the profile, whose form is identical to the square modulus of the Fourier transform of the surface $h(\mathbf{x})$ as calculated from the STM image.

[21]J. Wollschläger, E. Z. Luo, and M. Henzler, Phys. Rev. B **44**, 13 031 (1991).

[22]M. Horn, U. Gotter, and M. Helzler, J. Vac. Sci. Technol. B **6**, 727 (1988).

[23]J. Wollschläger, J. Falta, and M. Henzler, Appl. Phys. A **50**, 57 (1990).

[24]U. Köhler, O. Jusko, B. Müller, M. Horn-von Hoegen, and M. Pook, Ultramicroscopy **42-44**, 832 (1992).

[25]J. M. C. Thornton, A. A. Williams, J. E. Macdonald, R. G. van Silfhout, J. F. van der Veen, M. Finney, and C. Norris, J. Vac. Sci. Technol. B **9**, 2146 (1991).

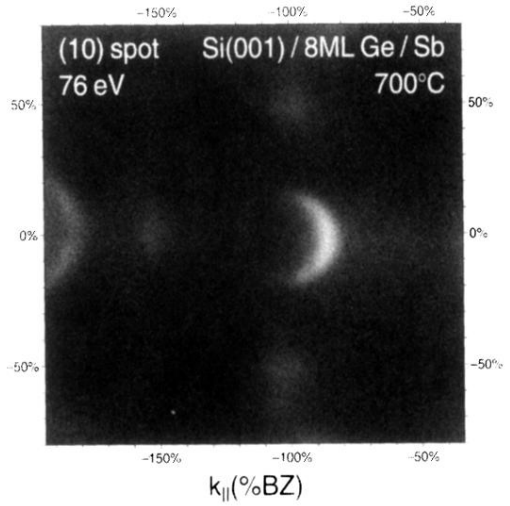

FIG. 1. Half-moon-shaped (10) spot at 74 eV after growth of 8 ML of Ge on Si(001) at 700 °C with Sb as a surfactant.

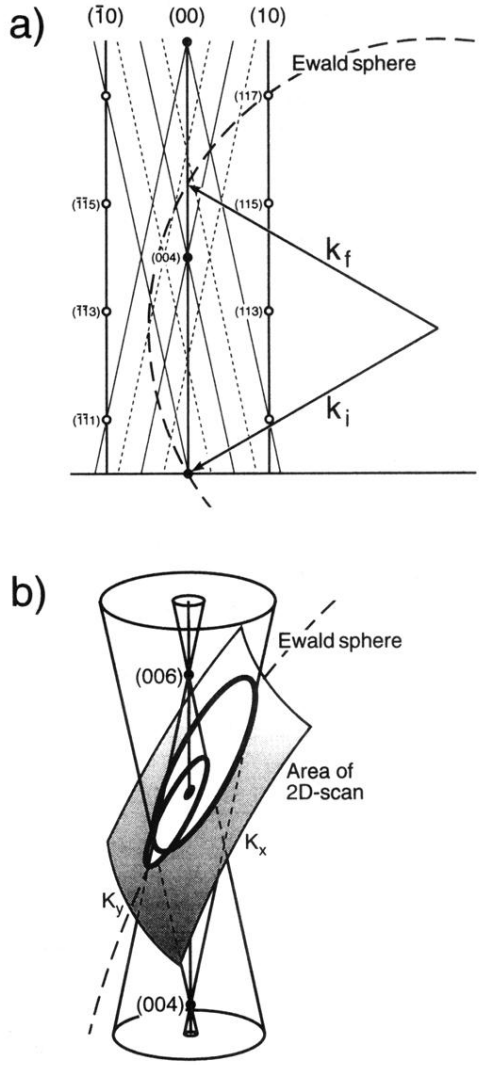

FIG. 10. Plot of the reciprocal space with the Ewald sphere for the geometry used with the external electron gun. Due to the 30° incident angle the LEED pattern is distorted by an extension of roughly a factor of 2 in the k_x direction. Additionally complicating is the dependence of k_z or the scattering phase S on the k_x component of the scattering vector. This leads to a strong distortion of the rings to deformed ellipses since the LEED pattern of the 12° cones strongly depends on the phase S. The result is sketched in the lower part of the figure: two intersecting ellipses form, one from the upward opened cone and the other from the downward opened cone, in the reciprocal space.

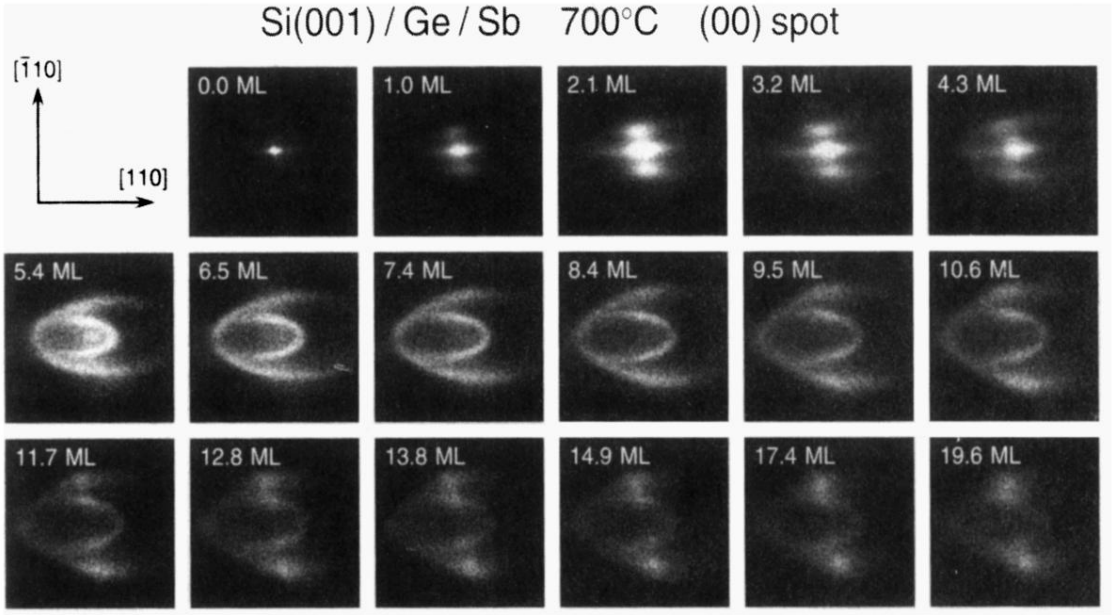

FIG. 11. A series of 2D scans reveals the formation of the 12° cones during the deposition. The LEED pattern is distorted due to the external gun geometry, as already shown in Fig. 10. The cones appear at ~5 ML and are visible up to ~12 ML of Ge. The size of the ellipses is increasing with coverage, indicating an increase of the facet tilt angle.

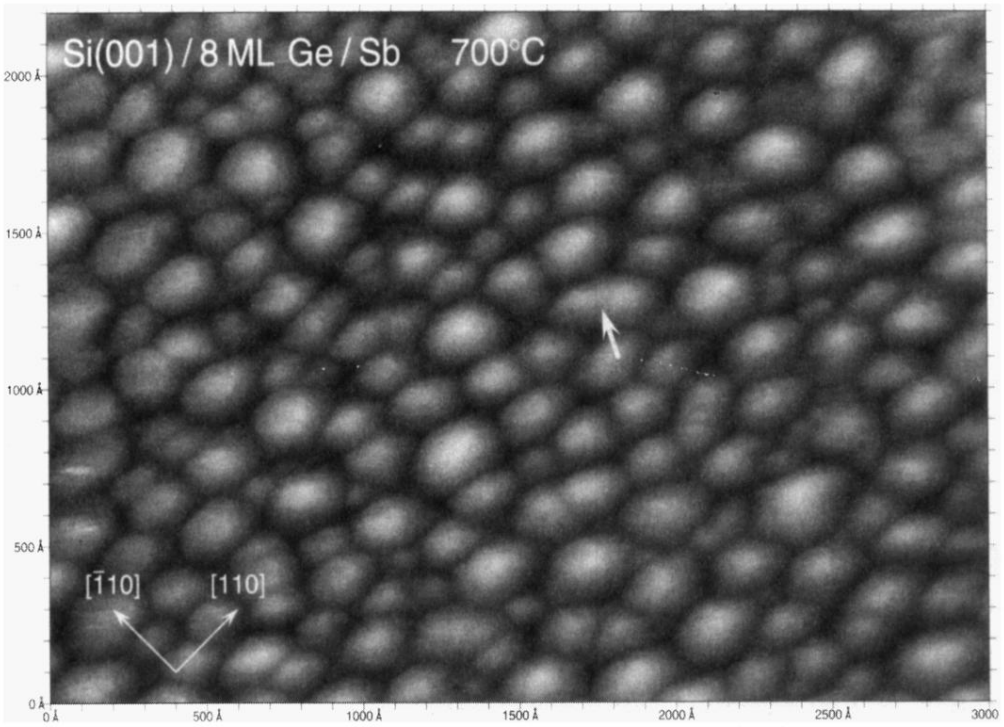

FIG. 14. STM image with a size of 3000×2200 Å after deposition of 8 ML of Ge on Si(001) with Sb as surfactant at 700 °C. The 12° cones cover the whole surface without any empty places. Areas between larger 12° cones are filled by very small islands.

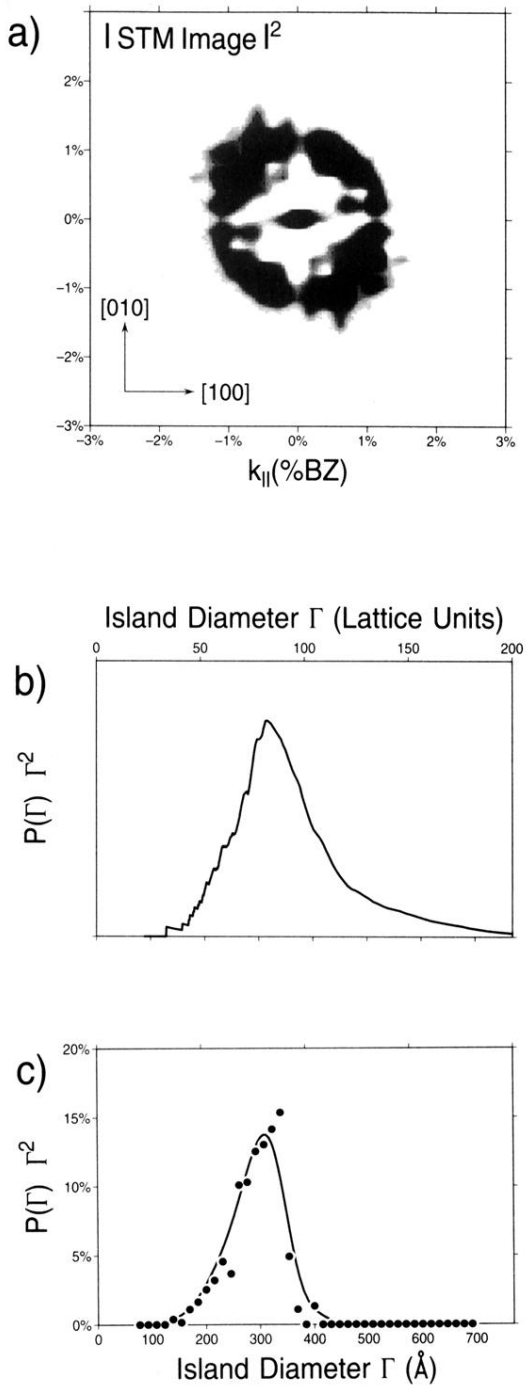

FIG. 15. The island-size and island-distance distribution is derived. (a) The square of the Fourier transform of the STM image shown in Fig. 14 reflects the 12° cone distance distribution and is identical to a LEED pattern close to the in-phase condition. The distribution shows maxima in the [100] directions, which is a hint for the preferred next-neighbor cone site. (b) The resulting isotropic distance distribution shows a very sharp maximum at a length of ~80 atoms, i.e., 300 Å. (c) The island-size distribution has been determined by estimating the size of any 12° cone visible in Fig. 14 and shows also very sharp maxima with a complete lack of 12° cones larger than 400 Å. These sharp-peaked distributions are a result of the equilibrium formation process of the 12° cones.

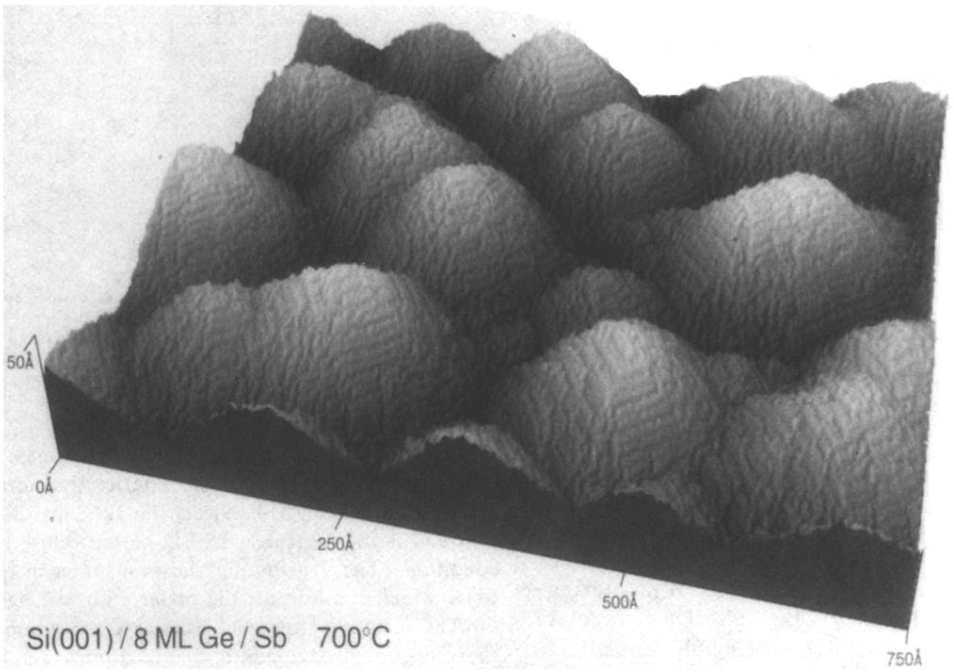

FIG. 16. The 12° cones are seen with atomic resolution in this perspective STM image with a size of 1000×700 Å (the height scale is exaggerated by a factor 2). The [105] facet (parallel to the border of the image) shows an unordered structure, whereas on the [117] facet even the double periodicity is observable. The 12° cones are not peaked but have a rounded top, reconstructed in a (2×1) structure.

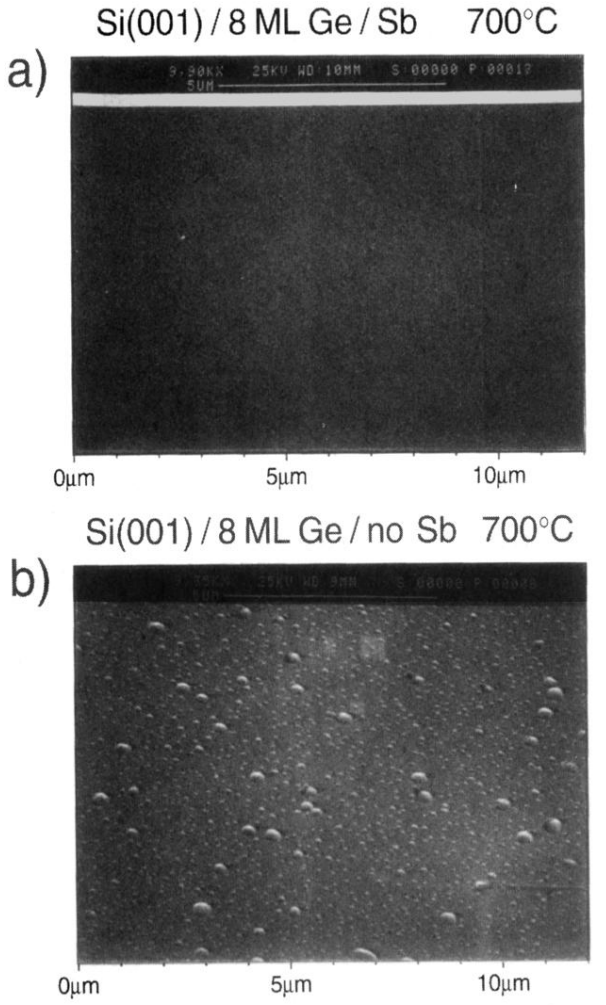

FIG. 17. (a) Using Sb as a surfactant during the deposition of Ge suppresses formation of large 3D clusters as shown in the SEM image of $\sim 10 \times 10$ μm size. The 12° cones are not visible due to the poor resolution of the instrument used. (b) Growth without surfactant results in the formation of a high number of 3D clusters with two different sizes of ~ 4000 and ~ 1000 Å diameter.

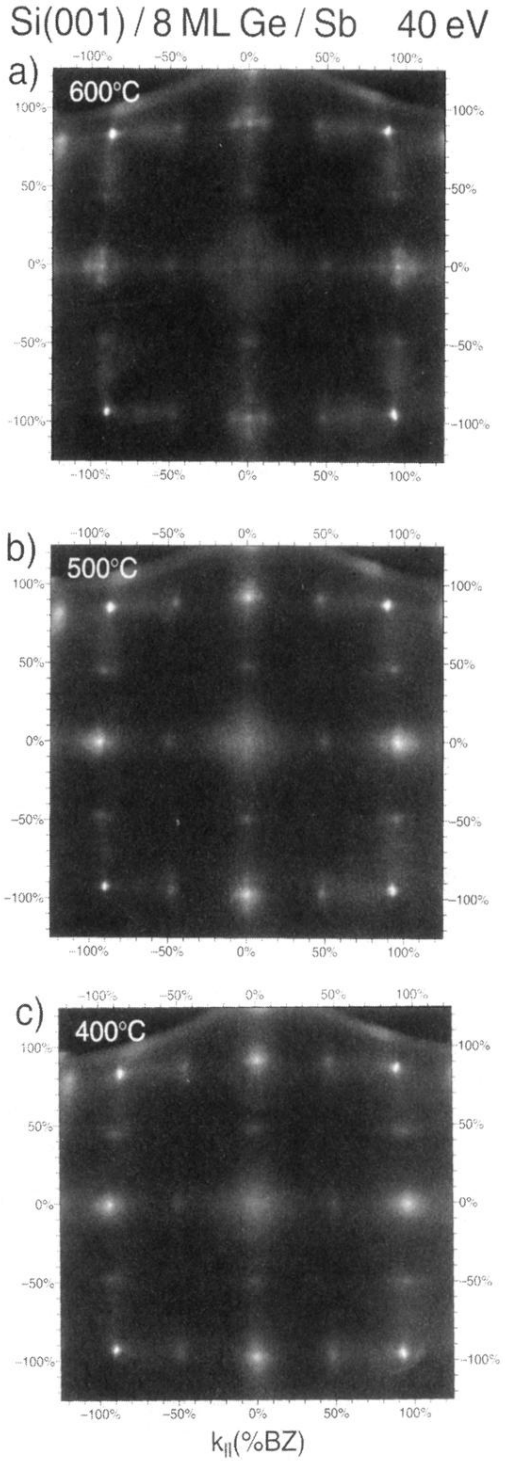

FIG. 18. Growth of 8 ML of Ge at lower temperatures results in quite different behavior. The sharp (11) spots indicate for all temperatures perfect epitaxial growth [41 eV is the in-phase condition of the (11) spots but the out-of-phase condition for the (00) spot]. The strong broadening of the (00) spot at all temperatures reflects the same lateral strong roughness of the Ge film. (a) At 600 °C growth temperature the LEED pattern shows a (8×2) reconstruction, as an ordered-surface morphology. (b) At 500 °C the LEED pattern still has some structure resembling the (8×2) seen at 600 °C. (c) At 400 °C and lower the broadening is featureless and could be described by a Lorentzian function.

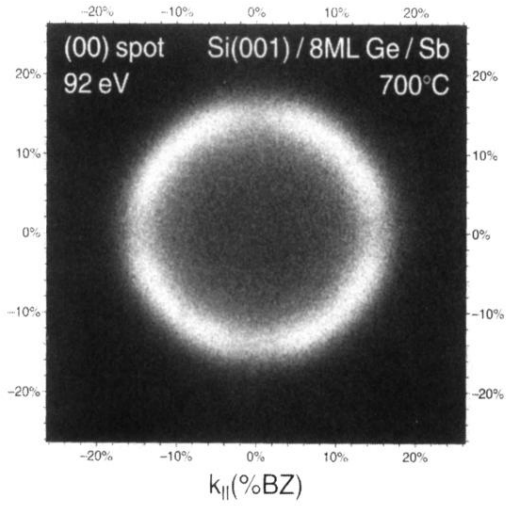

FIG. 2. The (00) spot at 90 eV shows a ringlike structure. The fourfold intensity variation on the perimeter is caused by dynamic scattering effects.

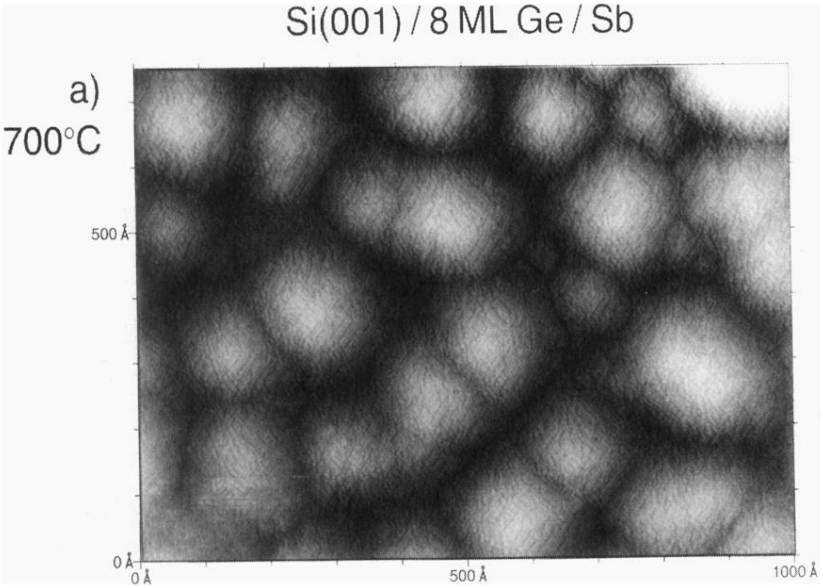

FIG. 21. The change from growth under equilibrium conditions to a growth under kinetic limitations is seen in this series of STM images for different growth temperatures. (a) At 700 °C growth temperature the STM shows the 12° cones. (b) At 600 °C the (2×8) becomes apparent in the STM. Even terraces on the same level are separated by one-atom-wide trenches in order to relieve strain. (c) At 530 °C the Ge film is quite rough and composed of small Ge terraces forming Ge islands with a size of ~400 Å.

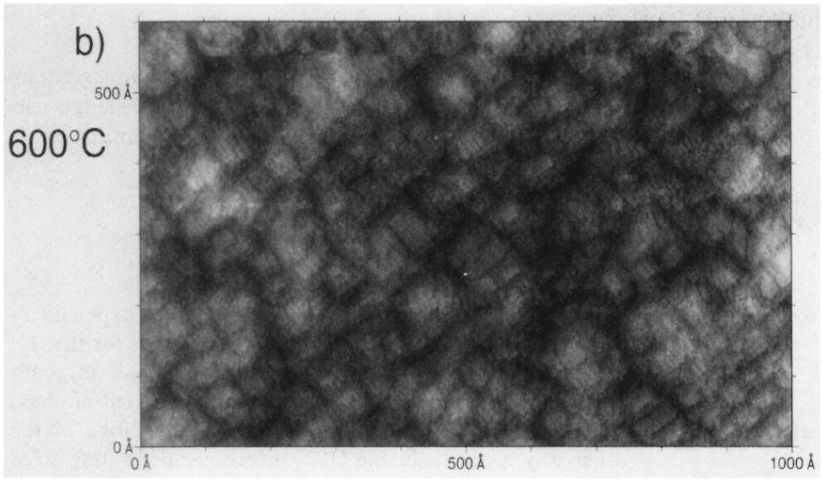

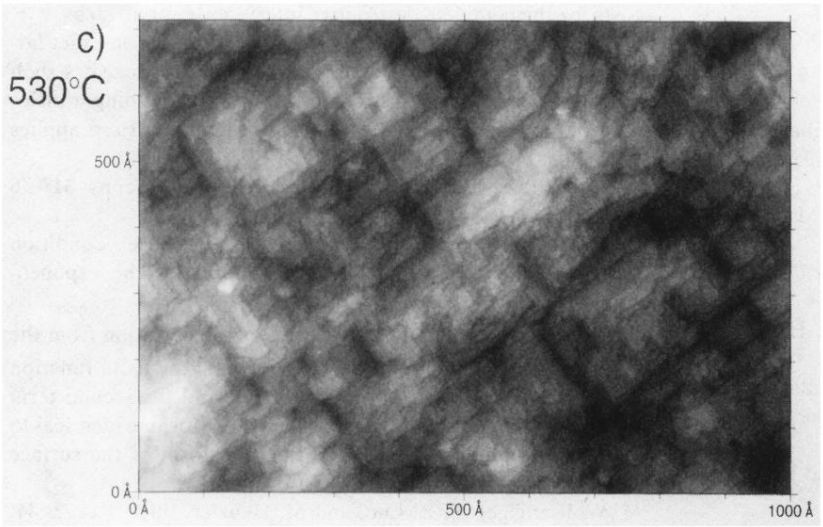

FIG. 21. (*Continued*).

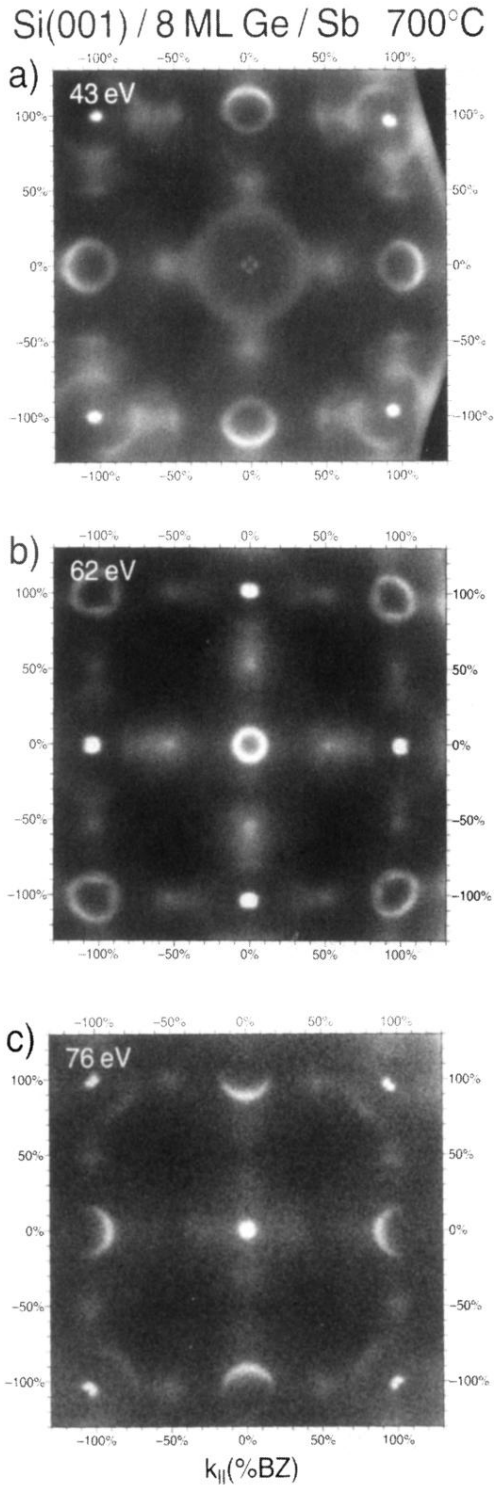

FIG. 3. All integer-order spots of the LEED patterns show the ringlike behavior. The diameter of the rings depends on the electron energy. (a) At 43 eV the (11) spots are bright and sharp due to their in-phase condition. The (10) spots show a ring as well as the (00) spot. The four faint spots in the center of the image are caused by an additional double periodicity on the [117] facets of the 12° cones. (b) At 62 eV the (10) spots have their in-phase condition. The (11) spots show a ring as well as the (00) spot. The size of the ring around the (00) spot has decreased. (c) At 76 eV the (00) spot is close to the in-phase condition. The (10) spots show a half-moon-shaped form caused by variations of the form factor of scattering.

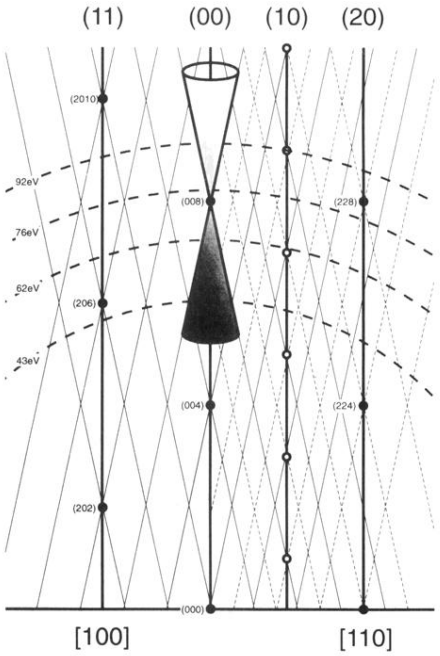

FIG. 4. The facet rods of the 12° cones on the (001) surface in the reciprocal space are plotted for two different azimuths. The in-phase conditions (the Bragg conditions) are plotted by dots and open circles. In the [100] direction [towards the (11) spots] no double periodicity occurs. The two nonequivalent steps in the [110] direction cause an inherent double periodicity (dashed lines) on these facets and thus double that many facet rods. The location of the 2D scans of Figs. 1–3 and the 1D scan of Fig. 7 are shown as dashed circle segments. The diffraction pattern of a 12° cone is in the reciprocal space; the cone is shaped like an ice-cream cone with an aperture angle of 24° (two times 12°). These reciprocal-space cones are opened upwards and downwards and located at any in-phase condition of scattering.

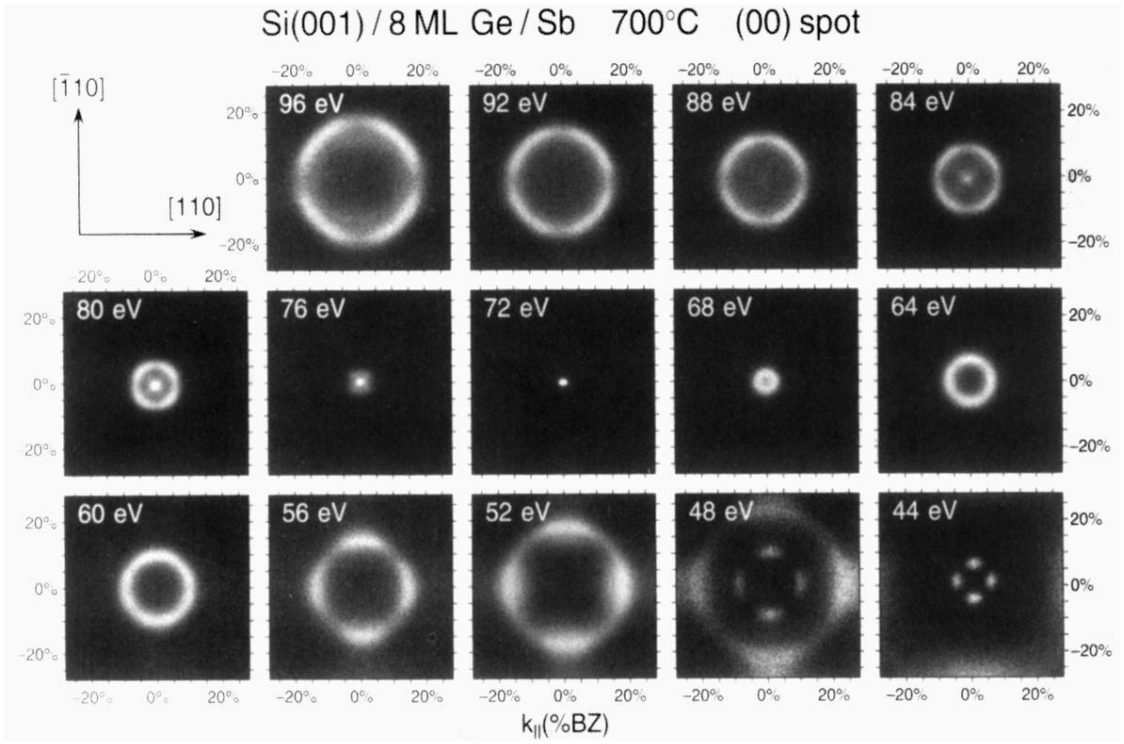

FIG. 5. The diameter of the ring around the (00) spot depends on the electron energy as shown in this series of 2D scans. The in-phase condition at 72 eV is clearly seen in the presence of the sharp central spot. The intensity of the ring is fourfold modulated by dynamic effects: at high energies weak maxima occur in the [100] directions, at low energies in the [110] directions. The four distinct intensity peaks at 48 and 44 eV are caused by the [117] facet, which has a double periodicity. Those peaks coalesce at the out-of-phase condition for single steps at 39 eV.